NASA CONTRACTOR REPORT

NASA CR-1055

THE SHOCK EXPANSION TUBE AND ITS APPLICATION AS A SONIC BOOM SIMULATOR

by Hugo E. Dahlke, George T. Kantarges, Thomas E. Siddon, and John J. Van Houten

Prepared by
LTV RESEARCH CENTER, WESTERN DIVISION
Anaheim, Calif.
for Langley Research Center

NATIONAL AERONAUTICS AND SPACE ADMINISTRATION • WASHINGTON, D. C. • JUNE 1968

NASA CR-1055

THE SHOCK EXPANSION TUBE AND ITS APPLICATION AS A SONIC BOOM SIMULATOR

By Hugo E. Dahlke, George T. Kantarges, Thomas E. Siddon, and John J. Van Houten

Issued by Originator as Technical Report No. 0-71200/7TR-125

Prepared under Contract No. NAS 1-5652 by
LTV RESEARCH CENTER, WESTERN DIVISION
Anaheim, Calif.

for Langley Research Center

NATIONAL AERONAUTICS AND SPACE ADMINISTRATION

For sale by the Clearinghouse for Federal Scientific and Technical Information
Springfield, Virginia 22151 – CFSTI price $3.00

THE SHOCK-EXPANSION TUBE
AND ITS APPLICATION AS A SONIC BOOM SIMULATOR

By Hugo E. Dahlke, George T. Kantarges
Thomas E. Siddon, and John J. Van Houten
LTV Research Center, Western Division
Ling-Temco-Vought, Inc.

SUMMARY

The generation of simulated sonic booms by mechanically bursting a pressurized diaphragm in a shock tube and expanding through an acoustic horn is described.

An analysis of the expansion tube phenomena is presented, the characteristics of the various wave and wave interactions in the tube-horn combination are established and projected in an x-t diagram. Mathematical expressions for these characteristic wave motions are computed for the expansion tube.

The simulator, installed on a trailer, consists of two shock tube driver sections, each 12 feet long coupled to an exponential horn with a mouth diameter of 13 feet and a lower cutoff frequency of 50 Hz. A variable time delay circuit provides a controllable period between the bursting of the two diaphragms.

The simulator can generate double blast waves with a maximum peak pressure of 27 psf (156 dB Ref. 2×10^{-4} dynes/cm^2) at 10 feet from the horn (on axis) using static pressure of 30 psig. The boom duration is variable from 10 to 600 msec.

The performance of the simulator was evaluated at Edwards Air Force Base by NASA personnel. Subjective data were obtained for quantitative evaluation. Structural response measurements on two instrumented houses were also collected. Data showing the shape of the blast wave pressure signatures, the radiation pattern on the ground, and blast wave pressure as a function of distance from the simulator are presented.

INTRODUCTION

The phenomenon of sonic boom generation by high speed aircraft has commanded considerable investigation and has resulted in extensive flight testing to obtain the necessary data. This procedure is both costly and time consuming, requiring the co-ordination of a large staff. The nature of the sonic boom problem is presented by Magliere and Carlson (Ref. 1) where the wave pattern is described and explained in terms of the pressure distributions to an observer on the ground. As discussed in the reference, the ear response is sensitive only to the two shock fronts and not to the slowly changing pressure between them.

It was, therefore, predicted that if two shock fronts were generated by conventional shock tubes with a variable time delay between blasts, a simulated sonic boom suitable for subjective evaluation would result.

The blast waves emanating from the two shock tubes would be expanded through a large horn to reduce the pressures and improve low frequency propagation.

The effects of subjective evaluation of sonic booms by artificial means were investigated by Zepler and Harel (Ref. 2). That study describes the use of a pressure transducer in the form of an earphone to generate the N-wave response. The effects of loudness versus rise time were investigated indicating that loudness is determined by the two pressure pulses while frequencies below 50 Hz are not important in the subjective analysis.

The need for a method of generating a simulated sonic boom was also indicated by the continued demand to study the reaction of community response to sonic booms and to investigate effects on the integrity of structures.

The advantages of the sonic boom simulating apparatus are evident by the relative simplicity of its operation, transportability, low cost of operation, and the ability to obtain variable intensities and time delays in the generation of sonic booms.

This report presents characteristics of the shock-expansion tube, i.e., the combination of a shock tube with an acoustic horn, and a description of the application of the device, which is designed to generate two weak shock waves and to serve as a controllable source of sonic booms.

CHARACTERISTICS OF THE SHOCK-EXPANSION TUBE

Acoustic pressure transients can be generated by the process of mechanically bursting a pressurized diaphragm as is accomplished by the shock tube technique. These pressure transients have potential applications associated with studies of physiological

and structural response to sonic boom pressures. The generation of transients having pressure amplitudes approaching those of sonic boom phenomena cannot be accomplished by direct application of conventional shock tube procedures. However, by coupling the shock tube with an acoustic horn, it has been possible to generate weak wave fronts with "jump pressures" more closely approximating those associated with sonic boom phenomena (i.e., of the order of 10 psf).* The horn is also necessary to provide for more efficient propagation and directional response of the generated shock front. Experiments have been performed to establish the validity of the analytical procedures. A discussion of these experiments is presented in the following section.

Analysis of The Expansion Tube, The x-t Plane

The expansion tube system, or shock tube-acoustic horn combination, is designed to operate by pressurizing a diaphragm with a gas and then bursting the stretched material by piercing. The experimental apparatus is shown in Figure 1. The mechanics of this process are summarized in the characteristics diagram of Figure 2. This diagram illustrates the various waves and wave interactions which occur in the shock tube-horn combination. The location of a wave at a given time after the diaphragm was burst is depicted by the various characteristics in the x-t plane. The projection of wave motion on this plane is readily accomplished since predictable wave velocities are graphically represented by

* Considerable work has been reported in the area of strong shock system development by application of the expansion or shock tunnel. For example, see Trimpi and Collis (Ref. 3).

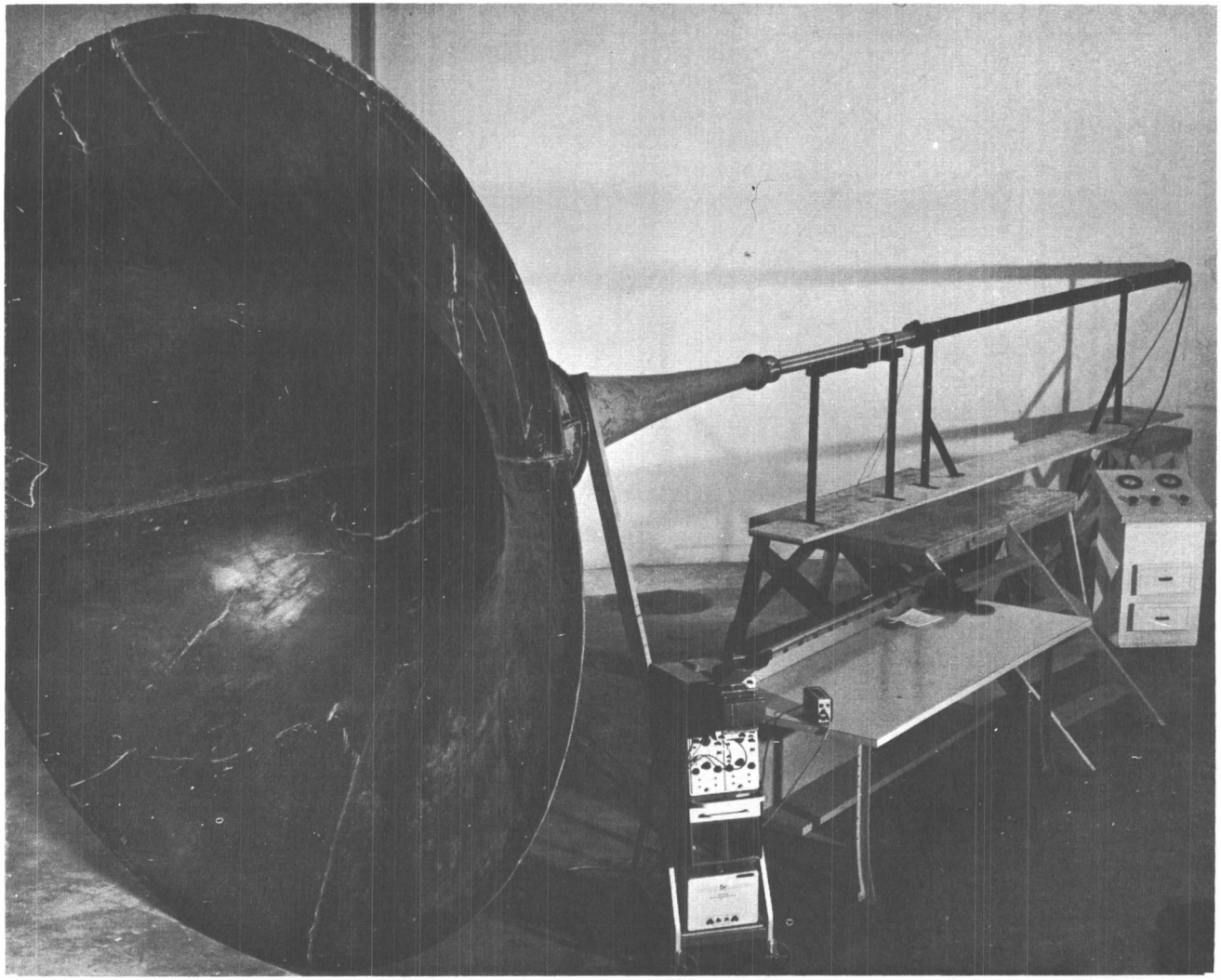

Shock Wave Expansion Tube

Figure 1

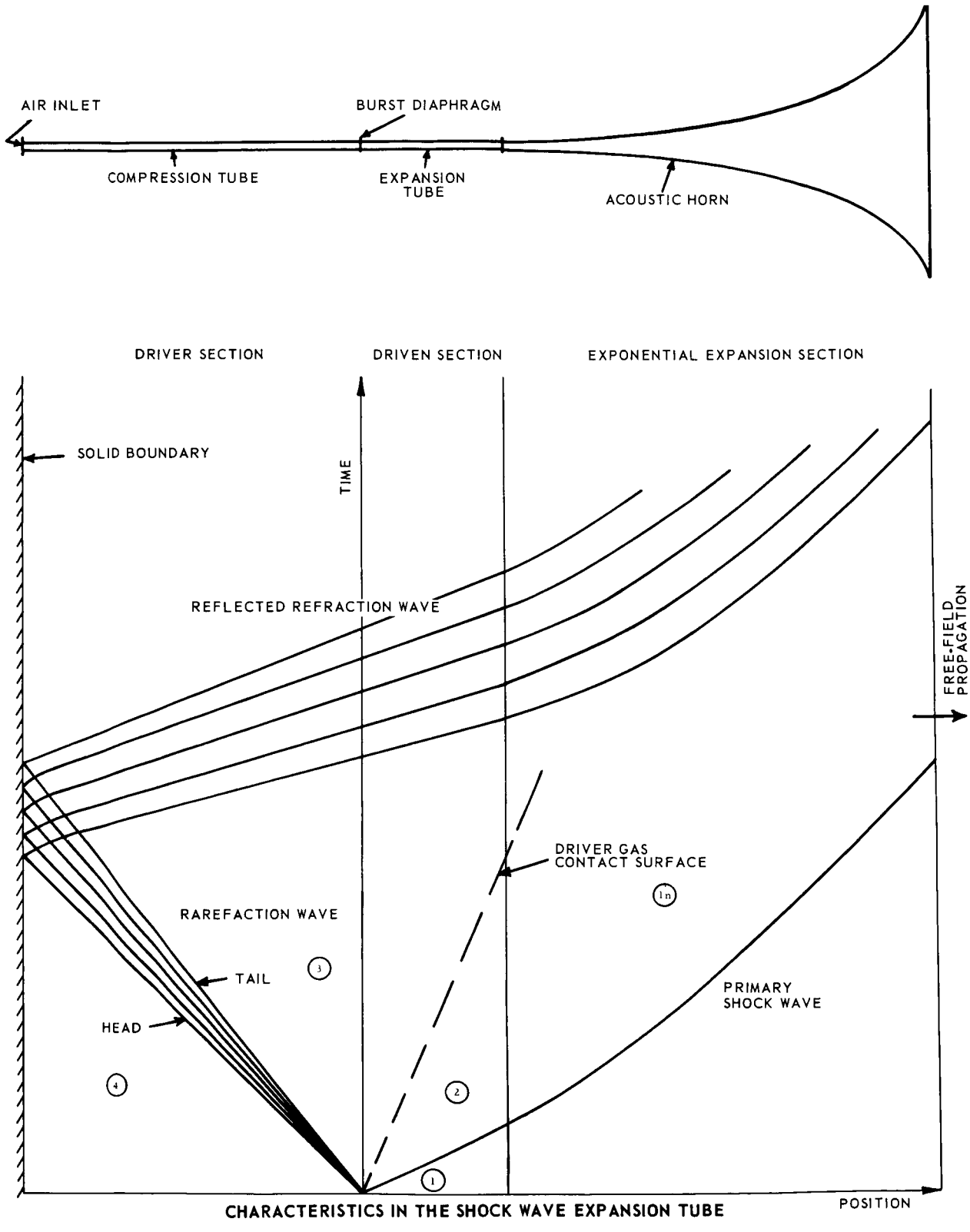

CHARACTERISTICS IN THE SHOCK WAVE EXPANSION TUBE

Figure 2

the slope of a line shown in the x-t diagram. Mathematical expressions for each characteristic of interest have been established by I. I. Glass (Ref. 4) and G. B. Whitham (Ref. 5). These expressions have been summarized in Figure 3 and outlined in detail in Appendix I.

The above mentioned wave characteristics have been computed by Glass for the shock tube application over a broad range of shock strengths. These computations have been expanded (Ref. 6) to include weak shock associated with the tube-horn combination. A description of weak shock behavior and computations for shock strength in the range of a few pounds/foot^2 are also presented in Reference 6.

The analytical method discussed by Whitham must be used in calculating the expansion through an acoustic horn in order to predict the wave characteristics in this region. Again, the pertinent analytical expressions are shown in Figure 3 and Appendix I. Computations have been made for wave motion in this expansion region at incremental changes of acoustic horn area. The strength or pressure of the primary wave is predicted from the wave speed by

$$P_{2\,1-n} = \left(\frac{\gamma-1}{\gamma-1}\right) \left[\frac{2\gamma M_1^2 - n}{\gamma-1} - 1\right] \quad \text{(See Appendix II)}$$

From the shock wave equations (Appendix I), it may be shown that

$$\frac{L_{1\,n}}{M_1 \to 1} \left(P_{4\,1} - 1\right) = 2 \left(P_{2\,1} - 1\right) = \frac{L_{1\,n}}{M \to 1} \left(P_{5\,1} - 1\right)$$

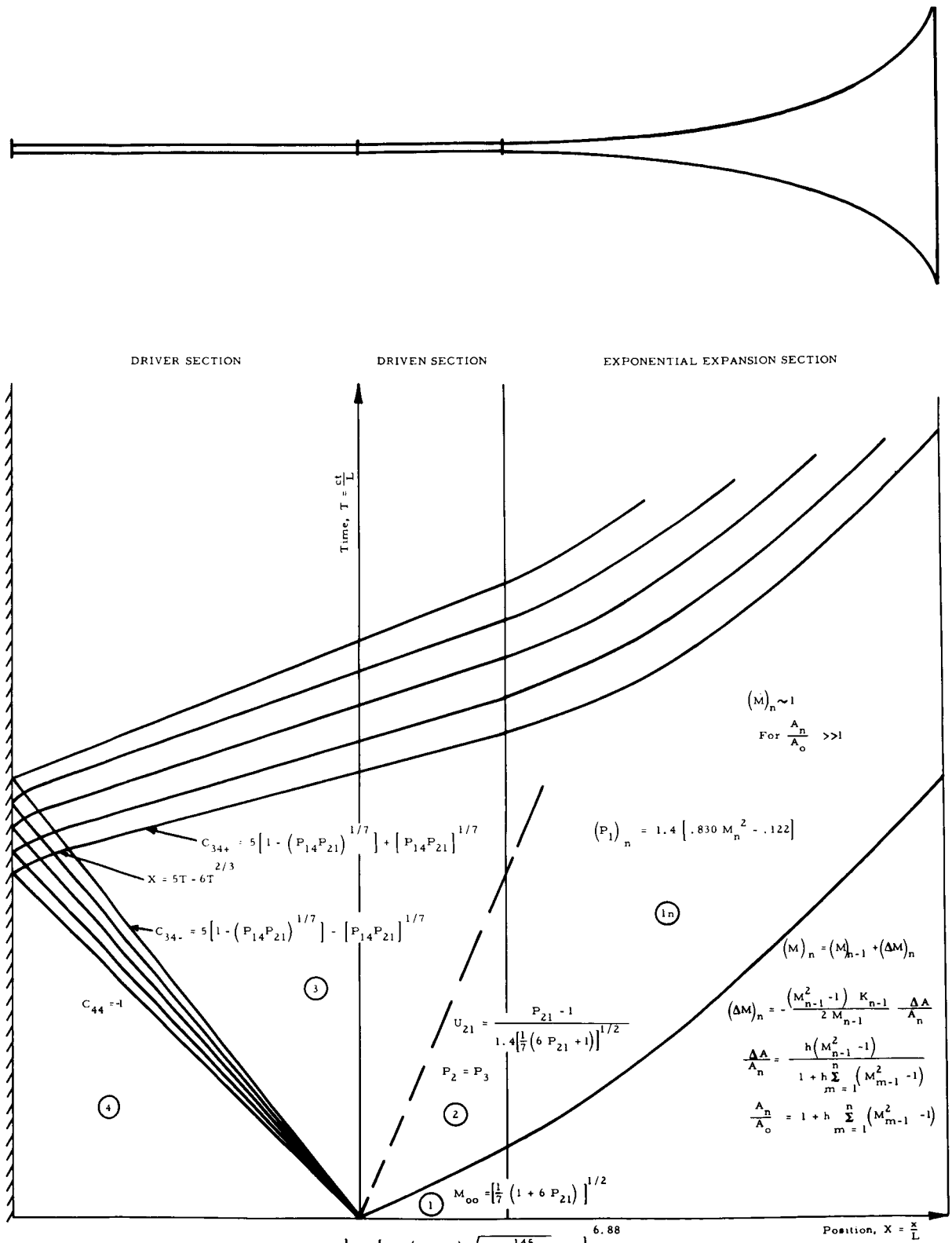

CHARACTERISTICS IN THE SHOCK WAVE EXPANSION TUBE

Figure 3

This relation is utilized in the extrapolation of the curves of Figure 1, (Appendix I), to very weak waves.

For the same limiting case, Whitham's solution for the expansion region (Ref. 5) reduces to

$$\underset{M_1 \to 1}{\lim} \left(\frac{M_{1-n} - 1}{M_{1-o} - 1} \right) = \left(\frac{A_o}{A_n} \right)^K$$

where $K = 0.5$ for weak shocks.

For an exponential horn, $A_n/A_o = e^{2x/h}$, and by use of the relation

$$\underset{M_1 \to 1}{\lim} \left(M_1 - 1 \right) = \frac{3}{7} \left(P_{21} - 1 \right)$$

the pressure at axial distance, x, from the horn mouth becomes

$$\underset{M_1 \to 1}{\lim} \quad \tilde{P}_{2-n} = \tilde{P}_{2-o} \, e^{-x/h}$$

where $\tilde{P}_{2-n} \alpha \left(P_{21-n} - 1 \right)$

which is compatible with the equivalent result from linear acoustics and has been utilized in the preparation of Figure 8.

Computation of the Parameters of the Expansion Tube

Tables 1 through 7 in Appendix I provides a complete listing of the characteristics and corresponding pressure for the

shock-expansion tube system. The information has also been presented in the form of graphs in Figures 1 through 5 of Appendix I. Complete x-t diagrams can be obtained using the tabulated and charted computations.

DESCRIPTION OF THE SIMULATOR

The simulator system consists of two shock tube driver sections of 12-foot lengths coupled into an exponential horn having a 13-foot diameter and 13-foot length. Its lower cutoff frequency is 50 Hz. Cellophane diaphragms separating the two pressurized driver sections from the horn are punctured by use of two electromagnetically driven plungers. A variable electronic time delay circuit provides a controllable period between the bursting of the two diaphragms thus providing a variable duration between the two blasts of the simulated sonic boom.

Figure 4 is a photograph showing the complete simulator mounted on a trailer. The essential components are the two driver tube sections, the horn, and the electronic and pneumatic control console. Storage tanks containing nitrogen used to pressurize the driver tube sections are visible near the console. The inside of each driver tube is lined with felt to attenuate the waves reflected from the end plate of the driver tube.

The diaphragm puncturing devices or plungers are mounted concentrically inside each driver tube behind the diaphragm as shown in Figures 5 and 6. The electric power required to operate the plunger consists of a 60 Hz pulse of approximately 100 ms duration and a peak-to-peak amplitude of 80 volts. The power is delivered

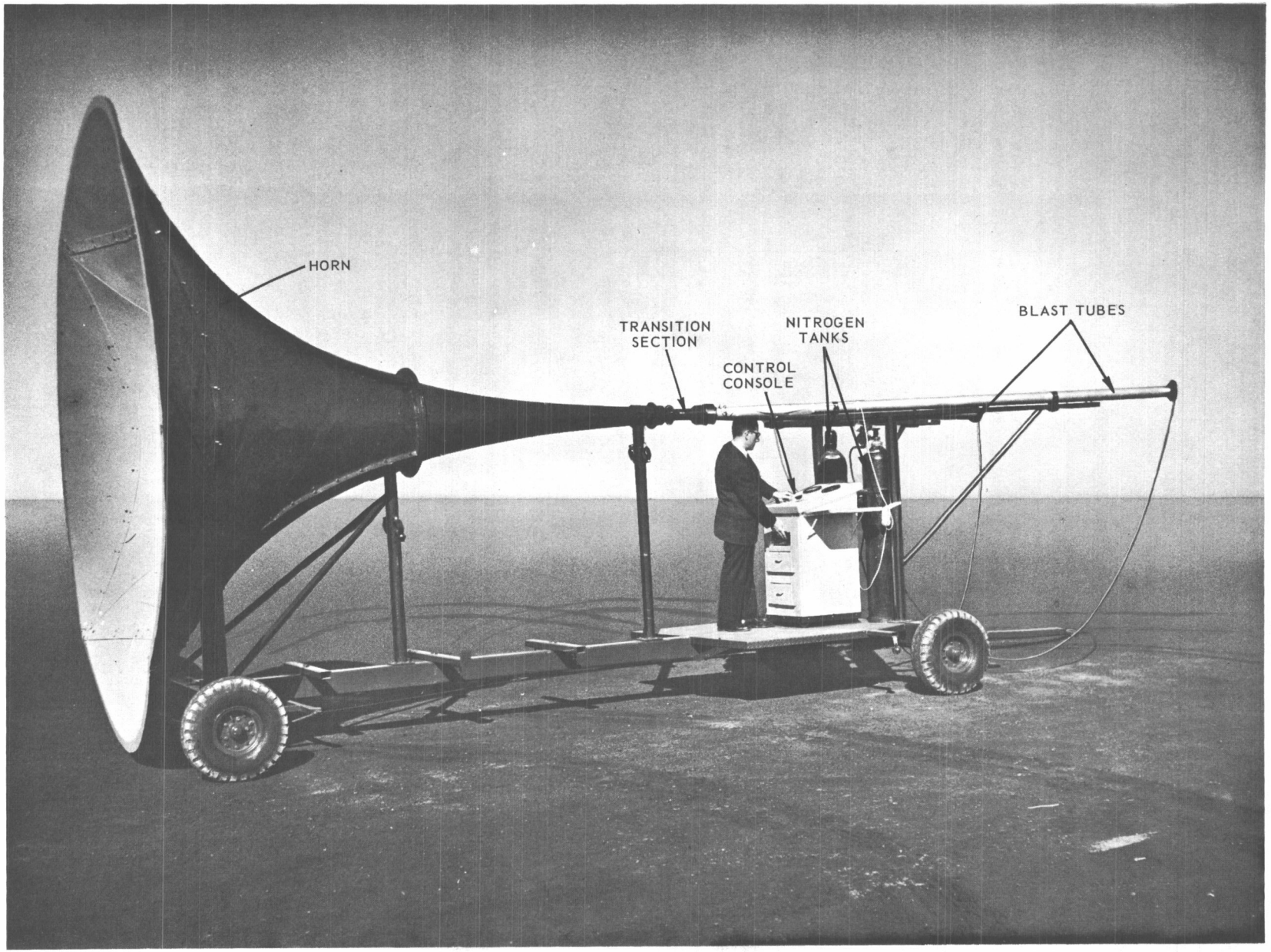

Fig. 4. Sonic Boom Simulator

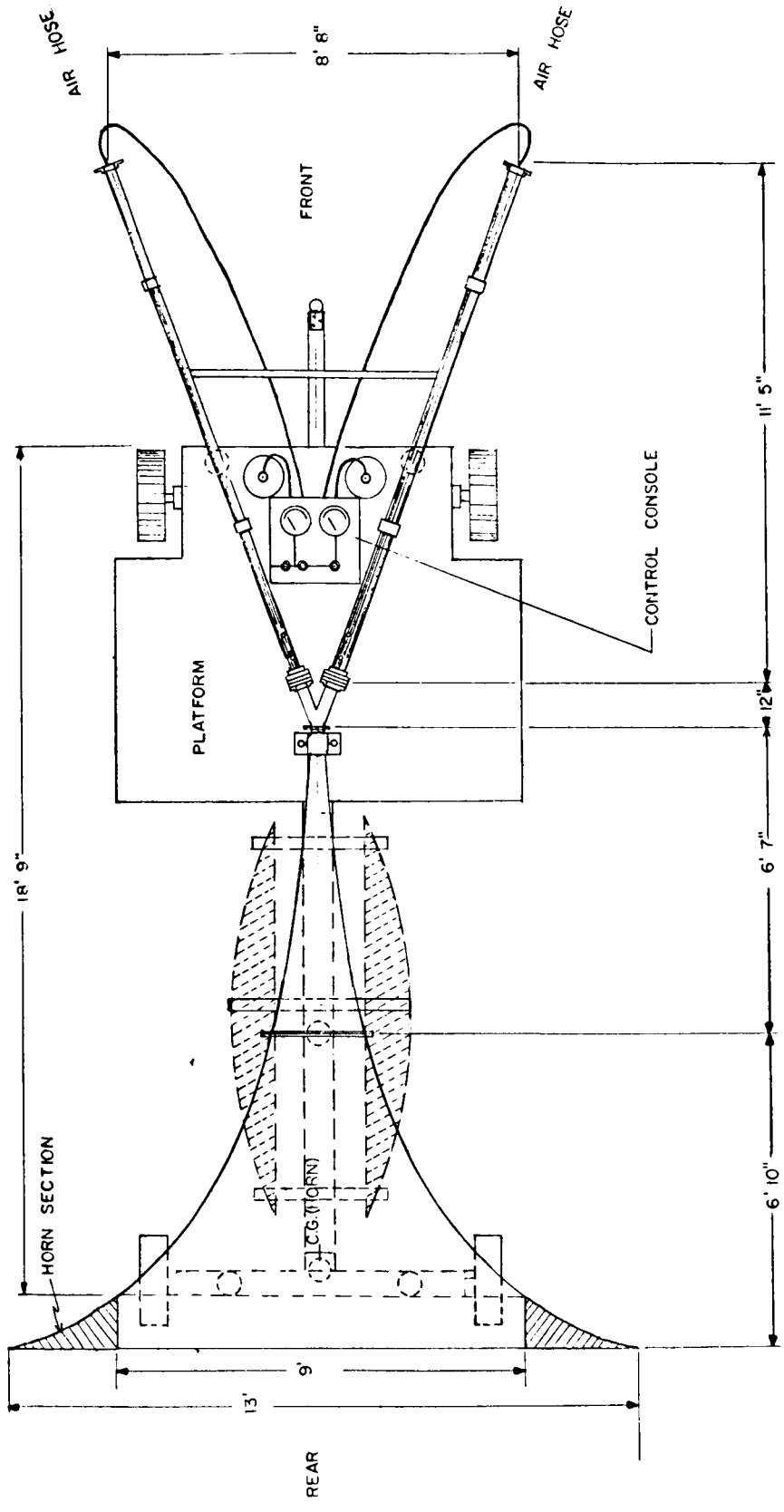

Fig. 5. Sonic Boom Simulator, Top View

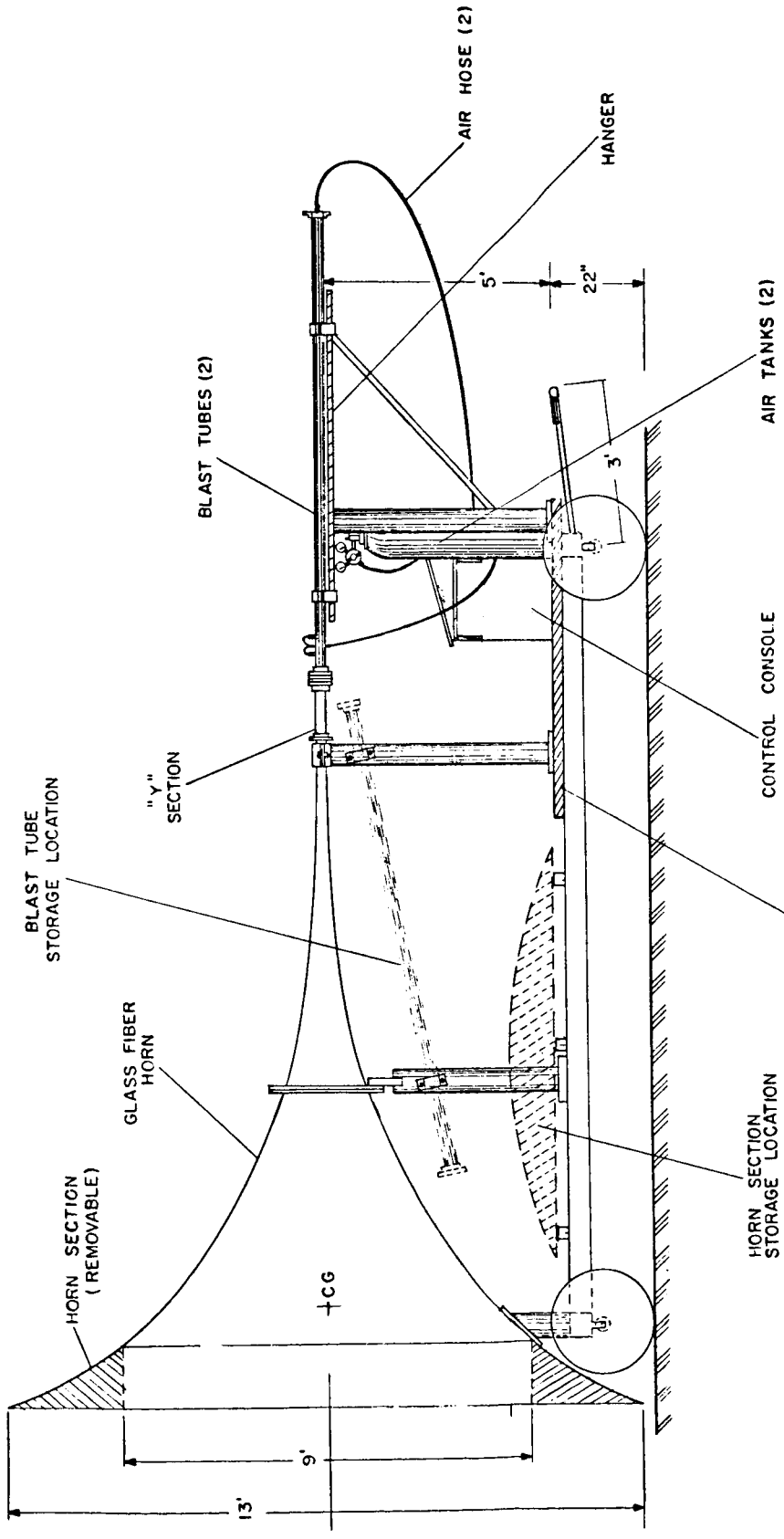

Fig. 6 . Sonic Boom Simulator, Elevation View

from the electronic driver located inside the console. The duration of the boom is variable from 10 to 600 msec. The required static pressure in the driver tube can be adjusted from 5 to 50 psi using compressed air or nitrogen.

The simulator generates pressure amplitudes which are of the same magnitude as those received from a supersonic aircraft.

A block diagram of the pneumatic and electronic instrumentation in the console is shown in Figure 7.

SPECTRAL ANALYSIS OF GENERATED WAVES

A determination of the frequency content or spectral analysis of the waves generated can be derived from the pressure time history by approximating the signature as an exponential blast wave of the form

$$P(t) = \left(1 - \frac{t}{t_o}\right) e^{-\frac{t}{t_o}}$$

A generalized transform can be made to establish the frequency content of this transient as shown in Figure 8. Experimentation has been conducted to verify the accuracy of the blast wave assumption (Ref. 7).

Due to the nonlinear nature of the problem, it is anticipated that the frequency content changes as a function of distance from the blast tube, and only approximates an exponential blast wave with constant period when the weak wave condition exists.

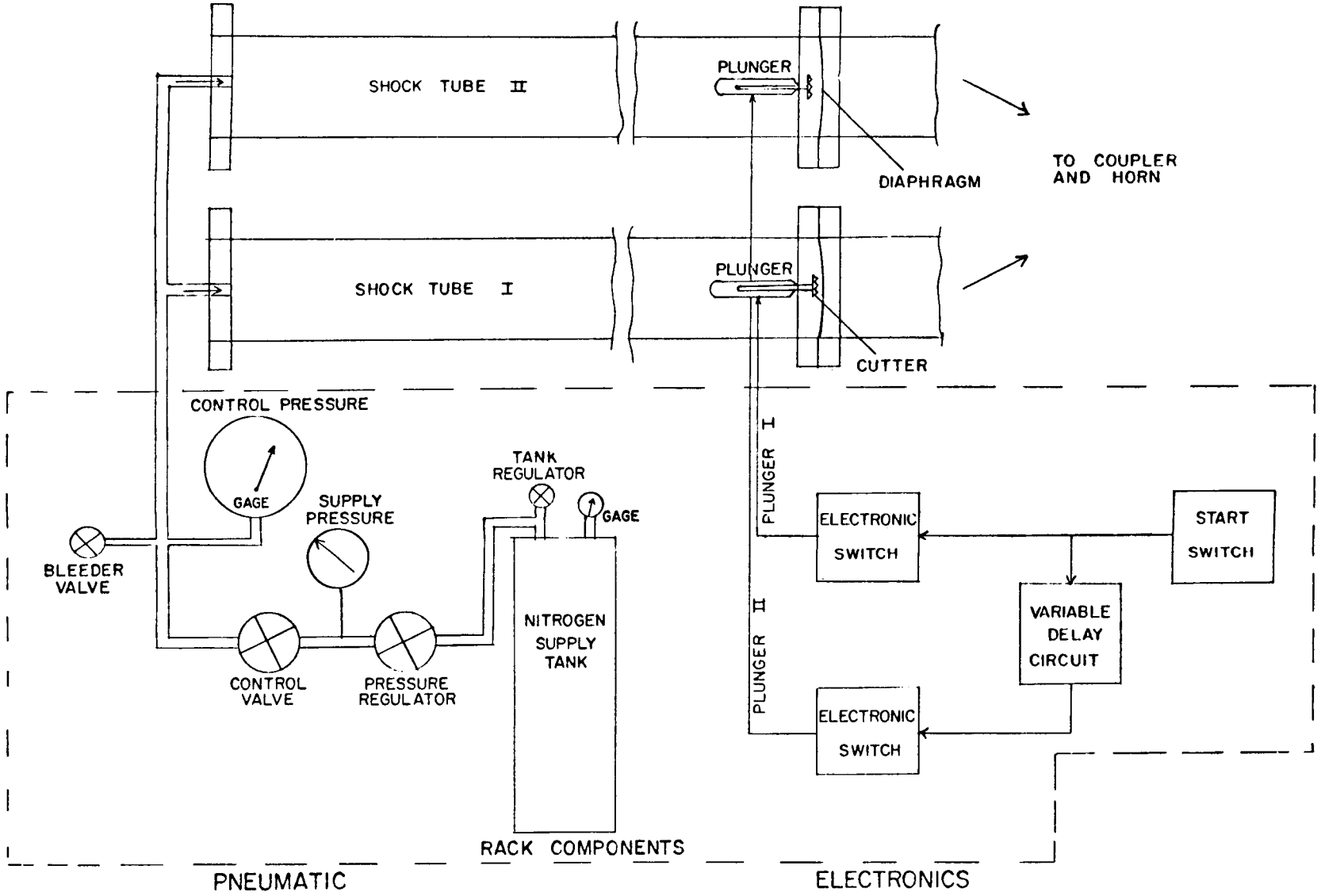

Fig. 7. Circuit Diagram of the Pneumatic and Electronic Complements of the Simulator

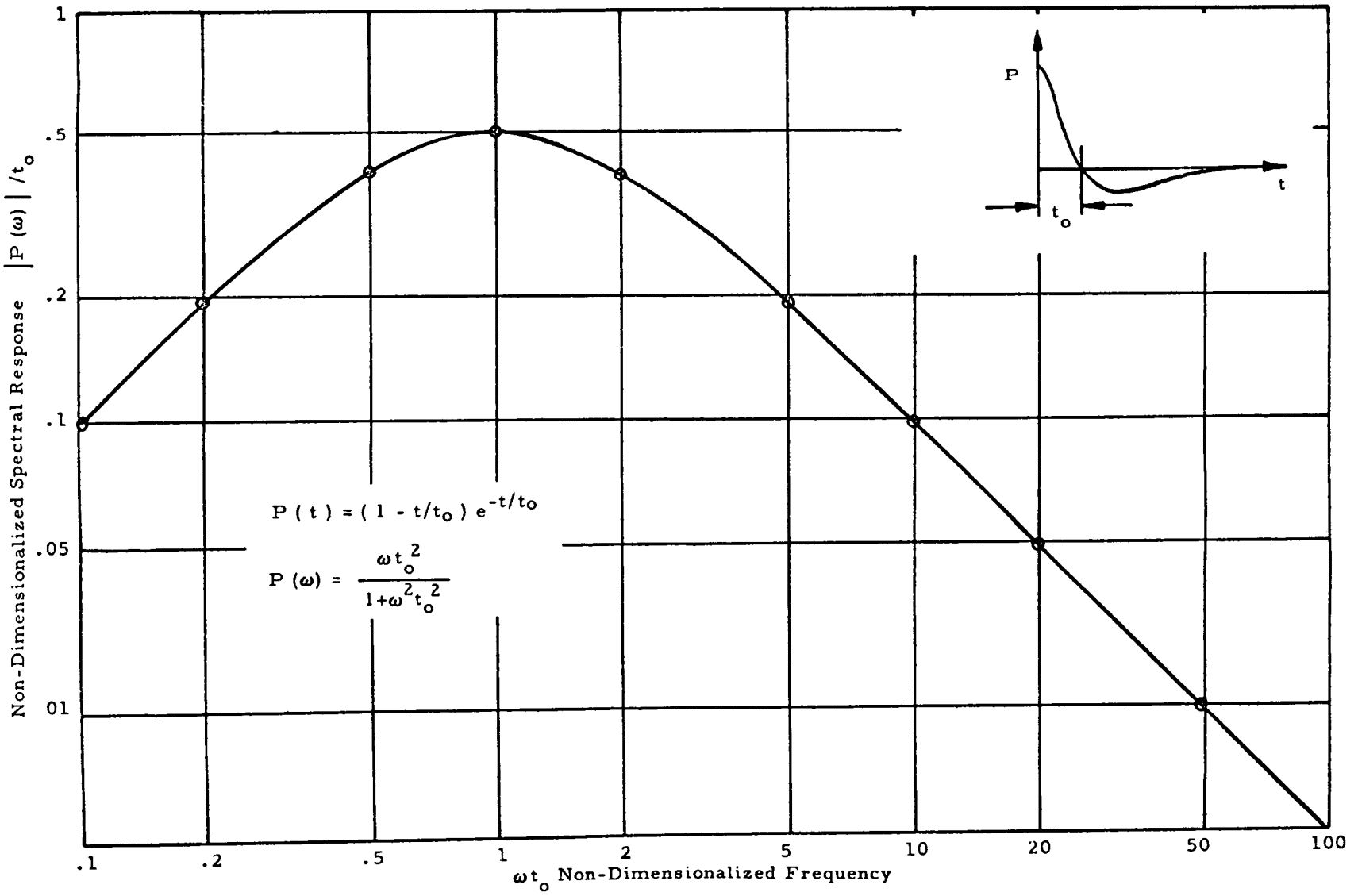

Fig. 8. Spectral Response for an Exponential Blast Wave

A variety of pressure signals can be generated using this basic system. For example, Figure 9 indicates the pressure time history at a position in front of the exponential horn. It is possible to vary the amplitude of each boom by suitable adjustment of the initial static pressure in the driver tubes. Tests have indicated, by measurements taken at lateral or off-axis positions of the horn, that some control of a variation of the rise time is achieved in this manner. Depending on the location, pressures above 25 psf have been achieved over a rather large area around the exit of the horn.

The pressure signatures in Figure 9 closely approximates the subjective reaction to sonic boom phenomena of Reference 2. Analog simulation was performed in our laboratory in order to establish the transfer function required to provide this wave signature from a perfect N-wave transient. Figure 10 indicates the result of this experiment. The input wave signature was an ideal N-wave which transformed to a transient very similar to that shown in Figure 9 by inserting a high pass filter designed with a lower cut-off frequency of approximately 35 Hz.

TEST DATA

The simulator was transported to Edwards Air Force Base to evaluate the effectiveness of the apparatus. Two types of tests were conducted by NASA personnel using the simulator.

1. Subjective data of a qualitative nature were obtained using personnel familiar with actual sonic booms generated in the area during extended sonic boom progress.

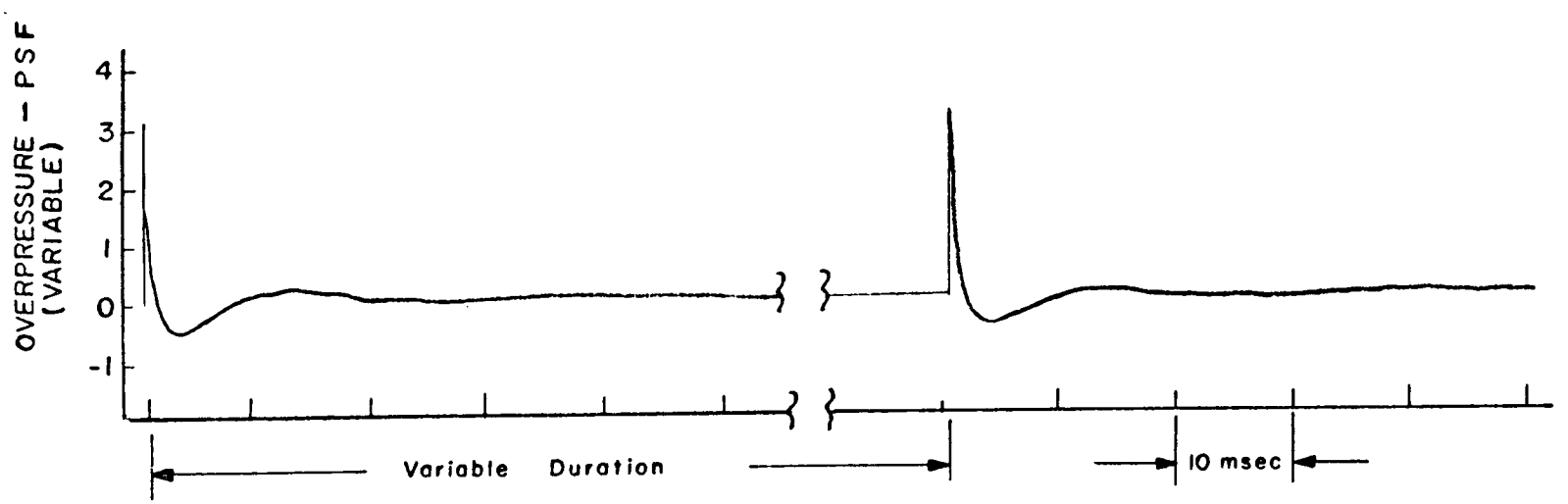

Fig. 9. Pressure Signatures Produced with the Sonic Boom Simulator

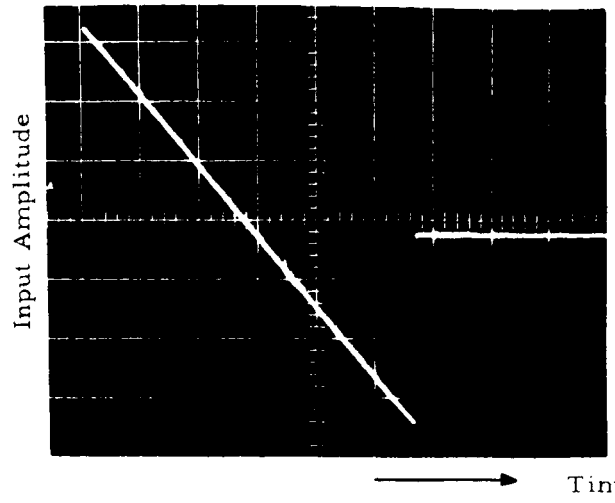

Input Waveform
to High Pass Filter

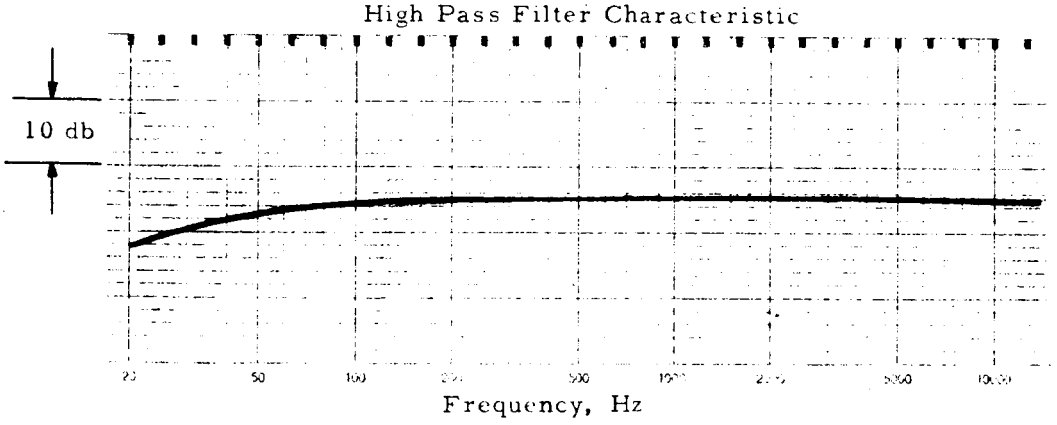

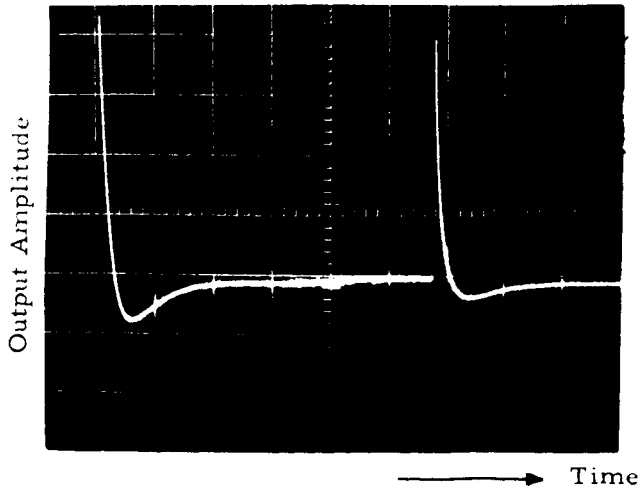

Output Waveform
of the Filter

Fig. 10 Analog Study – Subjective Simulation of Sonic Boom Phenomena

2. Data were obtained using the simulator on two instrumented houses built for the purpose of collecting information on structural response to sonic booms. The types of data obtained included acoustic impingement, strain and vibration on structural elements, and pressures in various parts of the two structures.

Overpressures or blast amplitudes that can be generated with the simulator are shown in Figure 11. The on-axis overpressure in psf is shown at a number of distances from the mouth of the horn for driver pressures (static pressure in the driver tubes) from 5 to 30 psig. A maximum peak pressure of 27.4 psf (156 dB ref. 0.0002 dyne/cm^2) at 10 feet distant was demonstrated for a driver pressure of 30 psig; while at 100 feet distant, a pressure of 5.4 psf was recorded. The microphones used were placed approximately 6 inches above the ground level and were shock mounted.

From the data, a contour of the sound pressure radiation from the mouth of the horn is plotted in Figure 12. A number of equal pressure contours in psf are shown as a function of lateral distance from the horn for a constant driver pressure of 10 psig.

Typical near field pressure signatures as measured 100 feet from the mouth of the horn are shown on the oscillograph records of Figure 13 for two lateral positions near the ground. Overpressures of approximately 0.90 psf were measured at a lateral distance of 15 feet, while at a lateral distance of 75 feet, the overpressure was in the order of 0.25 psf. Figure 14 is a photograph of the simulator during "firing" operations at the sonic

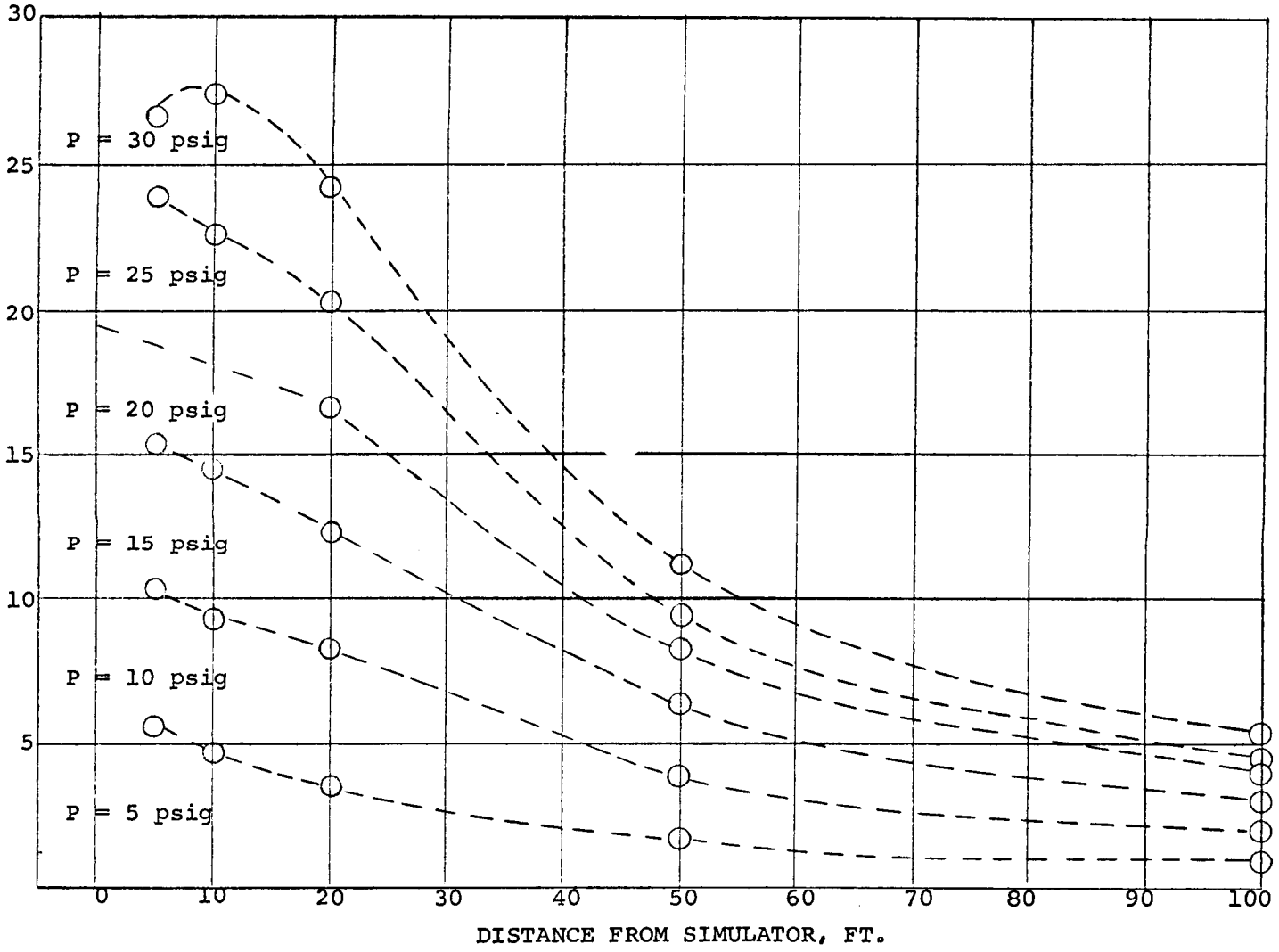

FIGURE 11 OVERPRESSURE OF BLAST WAVE Vs. DISTANCE FROM SIMULATOR FOR VARIOUS PRESSURES IN THE TUBE

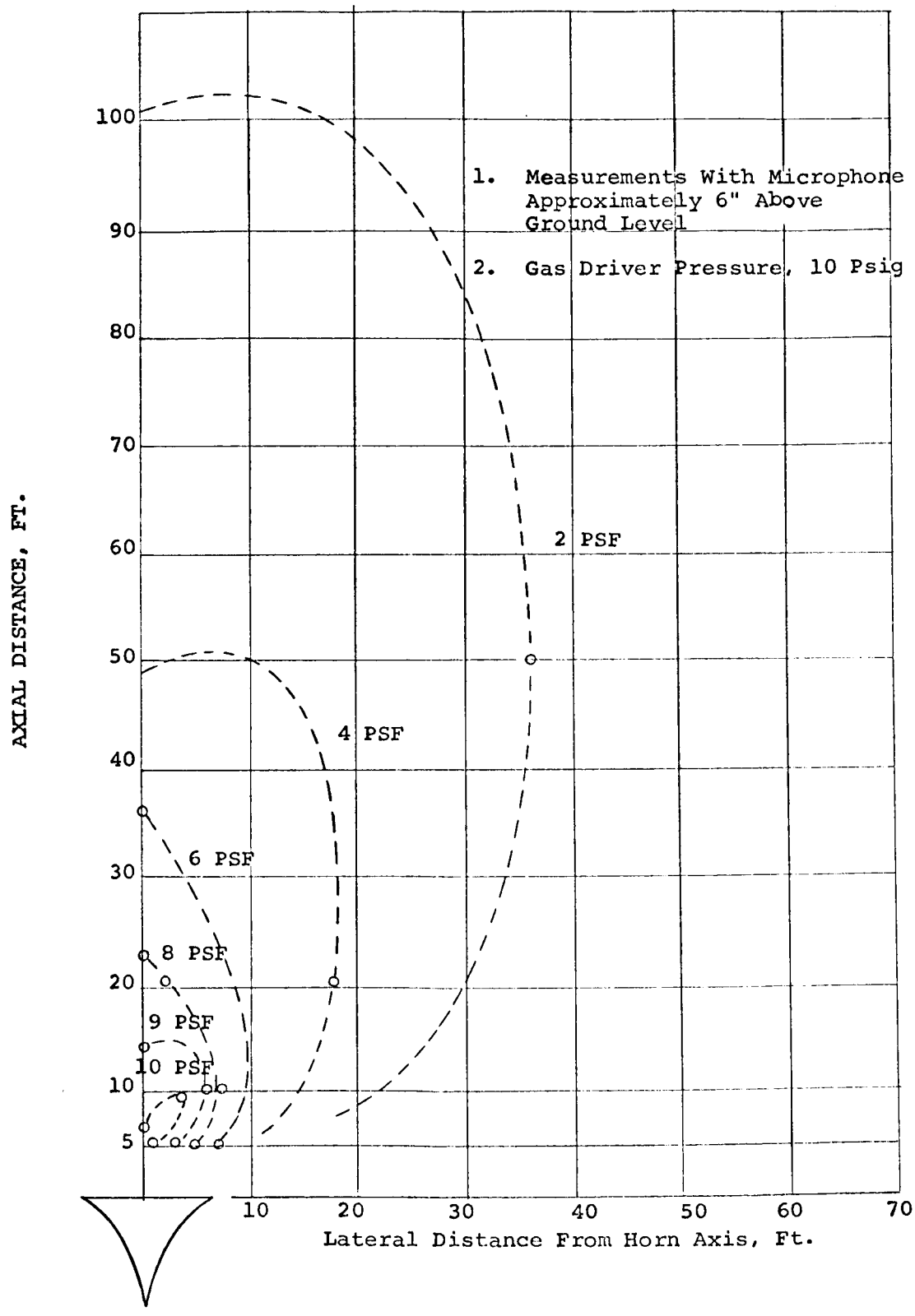

FIGURE 12 SONIC BOOM SIMULATOR - CONTOURS OF EQUAL OVERPRESSURE

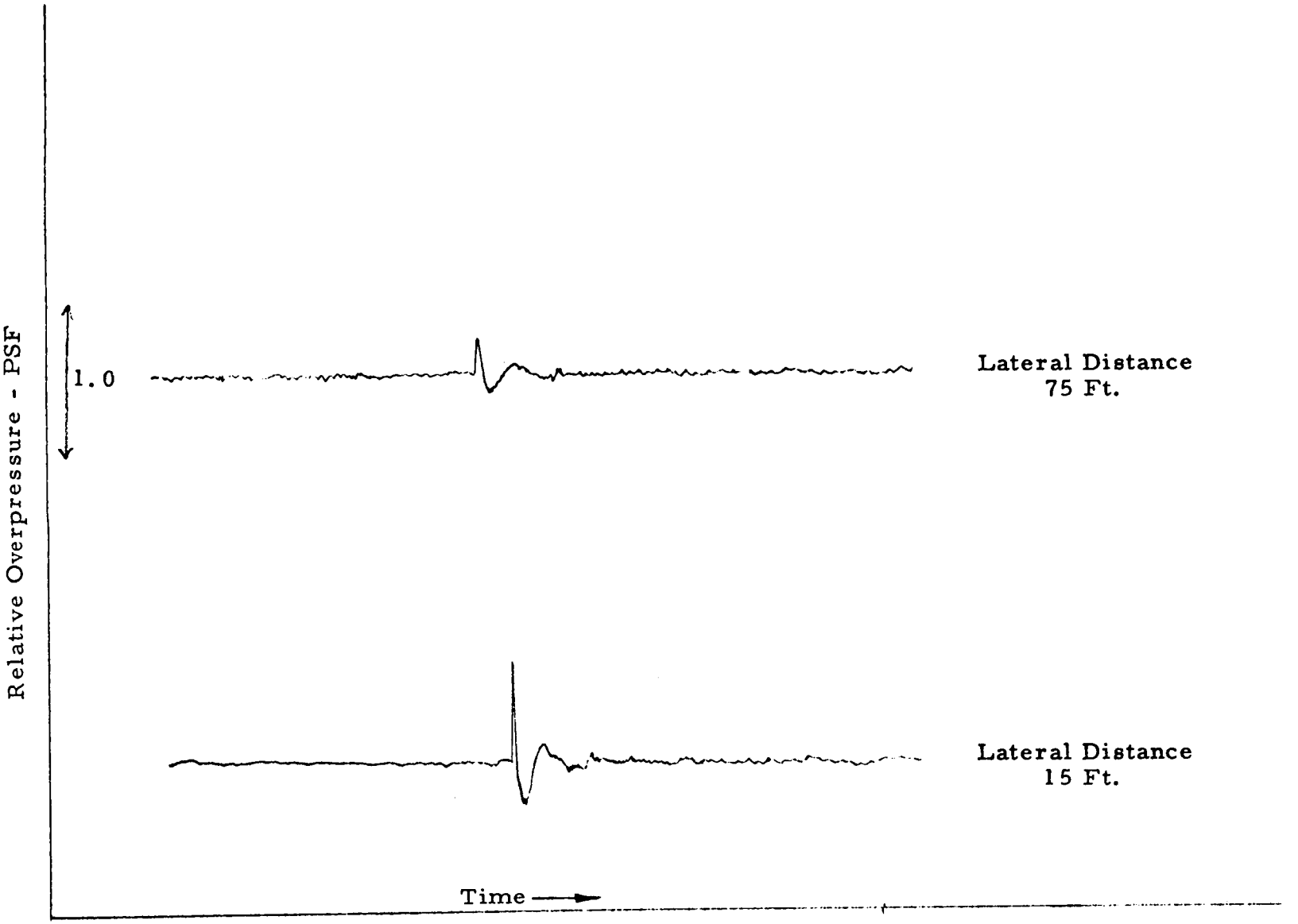

Fig. 13. Typical Pressure Signatures Generated by the Simulator at a Distance of 100 Ft. From the Horn.

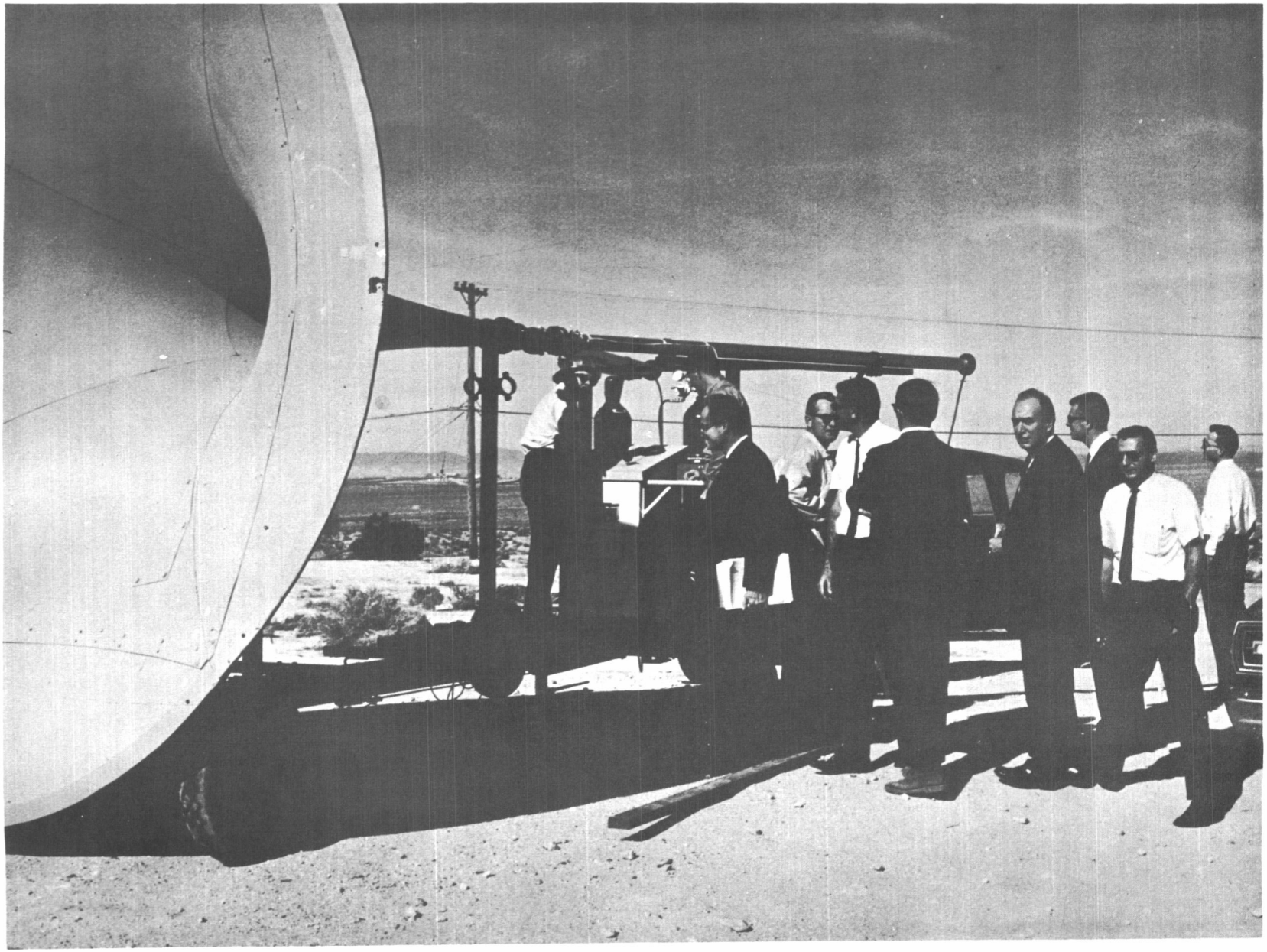

Fig. 14 Initial Simulation Test at Edwards Air Force Base

boom test area of Edwards Air Force Base.

The above data are presented here to indicate the type and approximate magnitude of pressure pulses encountered within the immediate area of the horn.

The simulator is currently being employed in environmental tests being conducted by the Department of Agriculture for animal husbandry research.

REFERENCES

1 D. J. Magleiri and H. W. Carlson, "The Shock Wave Noise Problem of Supersonic Aircraft in Study Flight," NASA Memorandum No. 3-4-59L (April 1959).

2 E. E. Zepler and J.R.P. Harel, "The Loudness of Sonic Booms and Other Impulsive Sounds," Journal of Sound and Vibration, Vol. 2, No. 3, pp 249-256 (1965).

3 R. L. Trimpi and L. B. Collis, "A Perfect Gas Analysis of the Expansion Tunnel a Modification to the Expansion Tube," NASA Technical Report R-223 (1965).

4 I. I. Glass, et al, "A Theoretical and Experimental Study of the Shock Tube," UTIA Report No. 2 (November 1953).

5 G. B. Whitham, "On the Propagation of Shock Waves Through Regions of Nonuniform Area or Flow," Journal of Fluid Mechanics, Vol. 4 (1958).

6 T. E. Siddon and J. J. Van Houten, "Characteristics of the Shock/Expansion Tube," Technical Report No. 0-71200/6TR-102, LTV Research Center, Western Division (July 1966).

7 R. Brown, et al, "Investigation of the Transient Response of Microphones, Quarterly Progress Report, October-December 1965," Technical Report No. 0-71200/6TR-88, LTV Research Center, Western Division (15 January 1966).

APPENDIX I

SHOCK/EXPANSION CHARACTERISTICS

The fundamental shock/expansion flow characteristics are summarized in the following material.

Initial driver-driven pressure ratio is given in terms of "strength," P_{21}, of the primary shock wave*

TABLE NO.

$$P_{41} = P_{21}\left[1 - \frac{(\gamma-1)(P_{21}-1)}{\sqrt{2\gamma}\sqrt{2\gamma+(\gamma+1)(P_{21}-1)}}\right]^{\frac{-2\gamma}{\gamma-1}} \qquad 1$$

Note that the gauge driving pressure is related to P_{41} by

$$\tilde{P}_4 = 14.7\ (P_{41} - 1)\ \text{psig} \qquad 1$$

For the constant area portion of the driven section, the shock wave Mach number is

$$M_{1-o} = \left[1 + (P_{21} - 1)\ \frac{\gamma+1}{2\gamma}\right]^{1/2} \qquad 2$$

The local flow Mach number immediately behind the shock wave (region 2) is expressed by

$$M_{2-o} = \frac{u_2}{a_2} = (P_{21} - 1)\left[\frac{2/\gamma}{\gamma P_{21}(\gamma P_{21} - P_{21} + \gamma + 1)}\right]^{1/2} \qquad 2$$

---

*Equations given here assume identical driver and driven gases, with the same initial temperature (i.e., $T_1 = T_4$, $\gamma_1 = \gamma_4$, $\therefore a_1 = a_4$). For more general relations, see Reference 4.

TABLE NO.

and the local flow Mach number behind the contact surface is

$$M_{3-o} = \frac{u_3}{a_3} = \frac{2}{\gamma-1}\left[(P_{21}P_{14})^{\frac{1-\gamma}{2\gamma}} - 1\right] \qquad 2$$

The particle velocity, u_2, normalized by a_1 is

$$U_{21-o} = \frac{u_2}{a_i} = (P_{21} - 1)\left[\frac{2/\gamma}{(\gamma+1)\ P_{21}+(\gamma-1)}\right]^{1/2} \qquad 3$$

The wave speed for the trailing edge of the rarefaction wave (normalized by a_4) is given by

$$C_{34\_} = \frac{1}{a_4}(u_3 - a_3) = (M_{3-o}-1)\ (P_{21}P_{14})^{\frac{\gamma-1}{2\gamma}} \qquad 3$$

and for the leading edge of the reflected rarefaction wave,

$$C_{34+} = \frac{1}{a_4}(u_3 + a_3) = (M_{3-o}+1)\ (P_{21}P_{14})^{\frac{\gamma-1}{2\gamma}} \qquad 3$$

The pressure ratio across the shock wave on normal reflection from a plane surface is given by

$$P_{52} = \frac{P_{21}\left(\frac{\gamma+1}{\gamma-1} + 2\right) - 1}{P_{21} + \frac{\gamma+1}{\gamma-1}} \quad ; \quad P_{51} = P_{52}P_{21} \qquad 4$$

and the Mach number of the reflected shock wave is

$$W_{21-o} = \frac{W_2 - u_2}{a_1} = \frac{P_{21}(\gamma-1) + 1}{\gamma\left[\frac{\gamma-1}{2\gamma}\left(\frac{\gamma+1}{\gamma-1}P_{21} + 1\right)\right]}^{1/2} \qquad 4$$

TABLE NO.

At station n within the expansion (horn) section, the Mach number becomes

$$(M)_n = M_{n-1} + (\Delta M)_n \qquad 5$$

Following Whitham's results (see Reference 5) for expansion flows, the incremental change in Mach number in the expansion region is

$$(\Delta M)_n = \frac{-(M_{n-1}^2 - 1)\ K\ (M)_{n-1}}{2M_{n-1}} \cdot \frac{\Delta A}{A_n}$$

where

$$\frac{\Delta A}{A_n} = \left[\frac{h\ (M_{n-1}^2 - 1)}{1 + h\left\langle \sum_{n=1}^{n} (M_{n-1}^2 - 1)\right\rangle}\right]$$

$$K(M)_{n-1} = 2\left[\left(1 + \frac{2}{\gamma+1}\ \frac{1-\mu^2}{\mu}\right)\left(2\mu + 1 + M_{n-1}^{-2}\right)\right]^{-1}$$

and

$$\mu^2 = \frac{(\gamma-1)\ M_{n-1}^2 + 2}{2\gamma M_{n-1}^2 - (\gamma-1)}$$

Finally, the expansion ratio at station n is

$$\frac{A_n}{A_0} = 1 + h\left\langle \sum_{n=1}^{n} (M_{n-1}^2 - 1)\right\rangle$$

Figures 1 through 5 of this appendix are graphical representations of the data contained in Tables 1 through 7.

APPENDIX I

TABLE I

P21	P12	P14	P41	P4 (PSIG)
1.0000	1.0000	1.0000	1.0000	0.
1.0500	0.9524	0.9067	1.1029	1.5127
1.1000	0.9091	0.8253	1.2117	3.1115
1.1500	0.8696	0.7539	1.3264	4.7982
1.2000	0.8333	0.6910	1.4473	6.5750
1.2500	0.8000	0.6352	1.5744	8.4440
1.3000	0.7692	0.5855	1.7080	10.4074
1.3500	0.7407	0.5411	1.8481	12.4674
1.4000	0.7143	0.5013	1.9950	14.6262
1.4500	0.6897	0.4654	2.1487	16.8863
1.5000	0.6667	0.4330	2.3095	19.2499
1.5500	0.6452	0.4036	2.4775	21.7196
1.6000	0.6250	0.3769	2.6529	24.2979
1.6500	0.6061	0.3526	2.8359	26.9873
1.7000	0.5882	0.3304	3.0266	29.7905
1.7500	0.5714	0.3101	3.2252	32.7101
1.8000	0.5556	0.2914	3.4319	35.7489
1.8500	0.5405	0.2742	3.6469	38.9097
1.9000	0.5263	0.2584	3.8704	42.1954
1.9500	0.5128	0.2437	4.1026	45.6088
2.0000	0.5000	0.2302	4.3437	49.1530
2.0500	0.4878	0.2177	4.5940	52.8311
2.1000	0.4762	0.2060	4.8535	56.6461
2.1500	0.4651	0.1952	5.1225	60.6012
2.2000	0.4545	0.1851	5.4013	64.6997
2.2500	0.4444	0.1757	5.6901	68.9449
2.3000	0.4348	0.1670	5.9891	73.3402
2.3500	0.4255	0.1588	6.2986	77.8890
2.4000	0.4167	0.1511	6.6187	82.5949
2.4500	0.4082	0.1439	6.9498	87.4615
2.5000	0.4000	0.1371	7.2920	92.4925
2.5500	0.3922	0.1308	7.6457	97.6915
2.6000	0.3846	0.1248	8.0111	103.0625
2.6500	0.3774	0.1192	8.3884	108.6094
2.7000	0.3704	0.1139	8.7780	114.3360
2.7500	0.3636	0.1089	9.1800	120.2466
2.8000	0.3571	0.1042	9.5949	126.3452
2.8500	0.3509	0.0998	10.0229	132.6360
2.9000	0.3448	0.0956	10.4642	139.1234
2.9500	0.3390	0.0916	10.9192	145.8119

APPENDIX I

TABLE II

P21	M10	M20	M30	P2 (PSFG)
1.0000	1.0005	0.	0.	0.
1.0500	1.0217	0.0347	0.0353	105.8400
1.1000	1.0425	0.0676	0.0696	211.6800
1.1500	1.0629	0.0988	0.1031	317.5200
1.2000	1.0829	0.1285	0.1358	423.3600
1.2500	1.1025	0.1569	0.1677	529.2000
1.3000	1.1218	0.1839	0.1990	635.0400
1.3500	1.1407	0.2099	0.2297	740.8800
1.4000	1.1594	0.2347	0.2597	846.7199
1.4500	1.1778	0.2586	0.2893	952.5590
1.5000	1.1958	0.2816	0.3183	1058.3999
1.5500	1.2136	0.3037	0.3468	1164.2399
1.6000	1.2312	0.3250	0.3749	1270.0799
1.650C	1.2485	0.3456	0.4026	1375.9199
1.700C	1.2655	0.3655	0.4299	1481.7599
1.750C	1.2824	0.3847	0.4568	1587.5999
1.8000	1.2990	0.4033	0.4834	1693.4399
1.8500	1.3154	0.4213	0.5096	1799.2799
1.9000	1.3316	0.4388	0.5355	1905.1199
1.9500	1.3476	0.4557	0.5611	2010.9599
2.0000	1.3635	0.4722	0.5865	2116.7998
2.0500	1.3791	0.4882	0.6115	2222.6398
2.1000	1.3946	0.5038	0.6364	2328.4798
2.1500	1.4099	0.5189	0.6609	2434.3197
2.2000	1.4250	0.5337	0.6853	2540.1597
2.2500	1.4400	0.5480	0.7094	2645.9997
2.3000	1.4548	0.5620	0.7333	2751.8396
2.3500	1.4695	0.5757	0.7570	2857.6796
2.4000	1.4840	0.5890	0.7806	2963.5195
2.4500	1.4984	0.6020	0.8039	3069.3595
2.5000	1.5126	0.6146	0.8271	3175.1995
2.5500	1.5267	0.6270	0.8501	3281.0394
2.6000	1.5407	0.6391	0.8730	3386.8794
2.6500	1.5546	0.6510	0.8957	3492.7194
2.7000	1.5683	0.6625	0.9182	3598.5593
2.7500	1.5819	0.6739	0.9406	3704.3993
2.8000	1.5954	0.6849	0.9629	3810.2392
2.8500	1.6088	0.6958	0.9851	3916.0792
2.9000	1.6221	0.7064	1.0071	4021.9192
2.9500	1.6353	0.7168	1.0290	4127.7591

APPENDIX I

TABLE III

P21	U21-0	C34+	C34-
1.0000	0.	1.0000	-1.0000
1.0500	0.0350	1.0280	-0.9580
1.1000	0.0685	1.0549	-0.9176
1.1500	0.1008	1.0808	-0.8788
1.2000	0.1319	1.1057	-0.8414
1.2500	0.1620	1.1298	-0.8053
1.3000	0.1910	1.1531	-0.7703
1.3500	0.2192	1.1757	-0.7365
1.4000	0.2464	1.1975	-0.7037
1.4500	0.2729	1.2188	-0.6719
1.5000	0.2987	1.2394	-0.6409
1.5500	0.3237	1.2595	-0.6108
1.6000	0.3481	1.2790	-0.5815
1.6500	0.3719	1.2981	-0.5529
1.7000	0.3951	1.3167	-0.5250
1.7500	0.4177	1.3349	-0.4977
1.8000	0.4399	1.3526	-0.4711
1.8500	0.4616	1.3700	-0.4450
1.9000	0.4828	1.3870	-0.4196
1.9500	0.5035	1.4036	-0.3946
2.0000	0.5239	1.4199	-0.3701
2.0500	0.5438	1.4359	-0.3461
2.1000	0.5634	1.4516	-0.3226
2.1500	0.5826	1.4670	-0.2995
2.2000	0.6015	1.4821	-0.2768
2.2500	0.6201	1.4970	-0.2545
2.3000	0.6383	1.5116	-0.2326
2.3500	0.6562	1.5260	-0.2110
2.4000	0.6739	1.5401	-0.1898
2.4500	0.6912	1.5540	-0.1689
2.5000	0.7083	1.5678	-0.1484
2.5500	0.7252	1.5813	-0.1281
2.6000	0.7418	1.5946	-0.1082
2.6500	0.7581	1.6077	-0.0885
2.7000	0.7743	1.6206	-0.0691
2.7500	0.7902	1.6334	-0.0500
2.8000	0.8059	1.6459	-0.0311
2.8500	0.8214	1.6583	-0.0125
2.9000	0.8367	1.6706	0.0059
2.9500	0.8518	1.6827	0.0241

APPENDIX I

TABLE IV

P21	W21-0	P51	P5 (PSIG)
1.0000	1.0005	1.0000	-0.0000
1.0500	0.9937	1.1021	1.5013
1.1000	0.9876	1.2085	3.0642
1.1500	0.9821	1.3189	4.6876
1.2000	0.9772	1.4333	6.3700
1.2500	0.9728	1.5517	8.1103
1.3000	0.9688	1.6740	9.9074
1.3500	0.9652	1.8000	11.7600
1.4000	0.9621	1.9297	13.6670
1.4500	0.9592	2.0631	15.6274
1.5000	0.9567	2.2000	17.6400
1.5500	0.9544	2.3404	19.7038
1.6000	0.9524	2.4842	21.8179
1.6500	0.9507	2.6314	23.9812
1.7000	0.9492	2.7818	26.1927
1.7500	0.9478	2.9355	28.4516
1.8000	0.9467	3.0923	30.7569
1.8500	0.9458	3.2522	33.1078
1.9000	0.9450	3.4152	35.5033
1.9500	0.9444	3.5811	37.9426
2.0000	0.9439	3.7500	40.4250
2.0500	0.9436	3.9217	42.9496
2.1000	0.9434	4.0963	45.5155
2.1500	0.9433	4.2736	48.1222
2.2000	0.9433	4.4537	50.7688
2.2500	0.9434	4.6364	53.4545
2.3000	0.9436	4.8217	56.1788
2.3500	0.9440	5.0096	58.9408
2.4000	0.9444	5.2000	61.7400
2.4500	0.9448	5.3929	64.5756
2.5000	0.9454	5.5882	67.4470
2.5500	0.9460	5.7860	70.3537
2.6000	0.9467	5.9860	73.2949
2.6500	0.9475	6.1884	76.2700
2.7000	0.9483	6.3931	79.2786
2.7500	0.9492	6.6000	82.3200
2.8000	0.9501	6.8091	85.3936
2.8500	0.9511	7.0203	88.4990
2.9000	0.9521	7.2337	91.6355
2.9500	0.9532	7.4492	94.8027

APPENDIX I

TABLE V

P21	(M)1	(M)2	(M)4	(M)8	(M)16	(M)32
1.0000	1.0005	1.0003	1.0002	1.0001	1.0001	1.0000
1.0500	1.0217	1.0150	1.0101	1.0068	1.0046	1.0031
1.1000	1.0425	1.0298	1.0203	1.0138	1.0093	1.0062
1.1500	1.0629	1.0448	1.0306	1.0208	1.0140	1.0095
1.2000	1.0829	1.0596	1.0408	1.0278	1.0188	1.0127
1.2500	1.1025	1.0740	1.0509	1.0347	1.0235	1.0159
1.3000	1.1218	1.0882	1.0608	1.0415	1.0282	1.0191
1.3500	1.1407	1.1019	1.0703	1.0481	1.0327	1.0221
1.4000	1.1594	1.1153	1.0797	1.0546	1.0371	1.0251
1.4500	1.1778	1.1283	1.0887	1.0608	1.0414	1.0281
1.5000	1.1958	1.1408	1.0975	1.0669	1.0456	1.0309
1.5500	1.2136	1.1528	1.1061	1.0729	1.0497	1.0337
1.6000	1.2312	1.1649	1.1145	1.0787	1.0537	1.0365
1.6500	1.2485	1.1769	1.1227	1.0843	1.0576	1.0392
1.7000	1.2655	1.1884	1.1307	1.0899	1.0614	1.0418
1.7500	1.2824	1.1996	1.1386	1.0954	1.0652	1.0444
1.8000	1.2990	1.2110	1.1463	1.1007	1.0689	1.0469
1.8500	1.3154	1.2218	1.1540	1.1060	1.0726	1.0495
1.9000	1.3316	1.2328	1.1615	1.1112	1.0762	1.0519
1.9500	1.3476	1.2434	1.1689	1.1164	1.0798	1.0544
2.0000	1.3635	1.2539	1.1761	1.1214	1.0833	1.0568
2.0500	1.3791	1.2644	1.1833	1.1265	1.0867	1.0592
2.1000	1.3946	1.2747	1.1904	1.1314	1.0902	1.0616
2.1500	1.4099	1.2849	1.1974	1.1363	1.0936	1.0639
2.2000	1.4250	1.2949	1.2044	1.1411	1.0969	1.0662
2.2500	1.4400	1.3048	1.2112	1.1458	1.1002	1.0685
2.3000	1.4548	1.3146	1.2179	1.1505	1.1035	1.0708
2.3500	1.4695	1.3243	1.2246	1.1551	1.1067	1.0730
2.4000	1.4840	1.3339	1.2311	1.1597	1.1099	1.0752
2.4500	1.4984	1.3433	1.2376	1.1642	1.1130	1.0774
2.5000	1.5126	1.3526	1.2440	1.1686	1.1161	1.0795
2.5500	1.5267	1.3618	1.2503	1.1730	1.1191	1.0816
2.6000	1.5407	1.3709	1.2565	1.1773	1.1221	1.0837
2.6500	1.5546	1.3799	1.2626	1.1816	1.1251	1.0858
2.7000	1.5683	1.3888	1.2687	1.1858	1.1280	1.0878
2.7500	1.5819	1.3975	1.2746	1.1899	1.1309	1.0898
2.8000	1.5954	1.4062	1.2805	1.1940	1.1337	1.0918
2.8500	1.6088	1.4147	1.2863	1.1980	1.1365	1.0937
2.9000	1.6221	1.4232	1.2920	1.2020	1.1393	1.0956
2.9500	1.6353	1.4315	1.2976	1.2059	1.1420	1.0975

APPENDIX I

TABLE VI

P21	(P21)1	(P21)2	(P21)4	(P21)8	(P21)16	(P21)32
1.0000	1.0012	1.0008	1.0005	1.0003	1.0001	1.0000
1.0500	1.0512	1.0351	1.0237	1.0160	1.0107	1.0072
1.1000	1.1013	1.0705	1.0479	1.0323	1.0217	1.0146
1.1500	1.1513	1.1069	1.0725	1.0490	1.0330	1.0222
1.2000	1.2014	1.1432	1.0972	1.0658	1.0443	1.0298
1.2500	1.2514	1.1792	1.1219	1.0824	1.0556	1.0374
1.3000	1.3015	1.2148	1.1461	1.0988	1.0666	1.0449
1.3500	1.3515	1.2500	1.1699	1.1150	1.0775	1.0522
1.4000	1.4016	1.2847	1.1933	1.1308	1.0882	1.0594
1.4500	1.4516	1.3186	1.2163	1.1462	1.0986	1.0664
1.5000	1.5017	1.3517	1.2387	1.1613	1.1088	1.0733
1.5500	1.5517	1.3837	1.2607	1.1762	1.1188	1.0800
1.6000	1.6018	1.4165	1.2824	1.1908	1.1286	1.0867
1.6500	1.6518	1.4494	1.3038	1.2051	1.1383	1.0932
1.7000	1.7019	1.4811	1.3249	1.2192	1.1478	1.0996
1.7500	1.7519	1.5122	1.3458	1.2331	1.1571	1.1059
1.8000	1.8020	1.5442	1.3665	1.2469	1.1664	1.1121
1.8500	1.8520	1.5748	1.3869	1.2605	1.1755	1.1182
1.9000	1.9021	1.6064	1.4072	1.2740	1.1846	1.1243
1.9500	1.9521	1.6372	1.4273	1.2874	1.1935	1.1304
2.0000	2.0022	1.6677	1.4472	1.3006	1.2024	1.1363
2.0500	2.0522	1.6984	1.4670	1.3137	1.2112	1.1422
2.1000	2.1023	1.7289	1.4867	1.3267	1.2199	1.1481
2.1500	2.1523	1.7594	1.5062	1.3396	1.2285	1.1539
2.2000	2.2024	1.7896	1.5256	1.3524	1.2370	1.1596
2.2500	2.2524	1.8197	1.5448	1.3650	1.2455	1.1653
2.3000	2.3025	1.8496	1.5639	1.3776	1.2539	1.1710
2.3500	2.3525	1.8794	1.5828	1.3900	1.2622	1.1765
2.4000	2,4026	1.9090	1.6016	1.4024	1.2704	1.1820
2.4500	2.4526	1.9385	1.6203	1.4146	1.2785	1.1875
2.5000	2.5027	1.9679	1.6388	1.4267	1.2866	1.1929
2.5500	2.5527	1.9970	1.6571	1.4386	1.2945	1.1982
2.6000	2.6028	2.0260	1.6753	1.4505	1.3024	1.2035
2.6500	2.6528	2.0549	1.6933	1.4622	1.3102	1.2087
2.7000	2.7029	2.0835	1.7111	1.4738	1.3178	1.2138
2.7500	2.7529	2.1120	1.7288	1.4852	1.3254	1.2189
2.8000	2.8030	2.1403	1.7463	1.4966	1.3329	1.2239
2.8500	2.8530	2.1684	1.7636	1.5078	1.3403	1.2289
2.9000	2.9031	2.1963	1.7808	1.5188	1.3477	1.2338
2.9500	2.9531	2.2240	1.7977	1.5298	1.3549	1.2386

APPENDIX I

TABLE VII

P21	(P2)1	(P2)2	(P2)4	(P2)8	(P2)16	(P2)32 (PSFG)
1.0000	2.4695	1.6546	1.0985	0.6996	0.3062	-0.0000
1.0500	108.4156	74.3997	50.2574	33.8382	22.7486	15.2852
1.1000	214.3618	149.1773	101.3972	68.3915	46.0227	30.9491
1.1500	320.3079	226.3503	153.5653	103.7051	69.8376	46.9894
1.2000	426.2540	303.1192	205.8485	139.2090	93.7899	63.1308
1.2500	532.2001	379.2419	258.0071	174.4719	117.5926	79.1766
1.3000	638.1462	454.6594	309.3520	209.2416	141.0628	95.0012
1.3500	744.0924	529.1922	359.6790	243.3720	164.0971	110.5321
1.4000	850.0385	602.5691	409.1491	276.8013	186.6480	125.7373
1.4500	955.9847	674.4500	457.7676	309.5003	208.7145	140.6118
1.5000	1061.9308	744.4443	505.2722	341.5436	230.3119	155.1700
1.5500	1167.8770	812.1291	551.7845	372.9650	251.4738	169.4328
1.6000	1273.8231	881.7373	597.8530	403.8045	272.2450	183.4290
1.6500	1379.7692	951.2762	643.0864	434.1482	292.6631	197.1848
1.7000	1485.7154	1018.4340	687.8492	464.0370	312.7690	210.7296
1.7500	1591.6615	1084.2792	732.0397	493.5309	332.5964	224.0832
1.8000	1697.6077	1152.0371	775.7187	522.6620	352.1758	237.2682
1.8500	1803.5538	1216.7508	818.9821	551.4929	371.5298	250.2989
1.9000	1909.4999	1283.6617	861.8654	580.0198	390.6790	263.1891
1.9500	2015.4460	1348.7921	904.4199	608.2837	409.6349	275.9466
2.0000	2121.3922	1413.4632	946.6413	636.2938	428.4088	288.5795
2.0500	2227.3381	1478.3320	988.5451	664.0567	447.0062	301.0903
2.1000	2333.2844	1542.8918	1030.1618	691.5808	465.4314	313.4824
2.1500	2439.2304	1607.4327	1071.4737	718.8687	483.6869	325.7573
2.2000	2545.1765	1671.4055	1112.4904	745.8860	501.7716	337.9137
2.2500	2651.1226	1735.0914	1153.2059	772.7369	519.6855	349.9508
2.3000	2757.0688	1798.4463	1193.6199	799.3138	537.4256	361.8686
2.3500	2863.0148	1861.4985	1233.7228	825.6487	554.9909	373.6656
2.4000	2968.9609	1924.2509	1273.5161	851.7375	572.3789	385.3382
2.4500	3074.9070	1986.6794	1312.9907	877.5677	589.5857	396.8844
2.5000	3180.8532	2048.7490	1352.1366	903.1606	606.6098	408.3033
2.5500	3288.7992	2110.5132	1390.9529	928.4830	623.4483	419.5940
2.6000	3392.7452	2171.9035	1429.4284	953.5536	640.0980	430.7516
2.6500	3498.6914	2232.9323	1467.5579	978.3526	656.5551	441.7738
2.7000	3604.6375	2293.5869	1505.3391	1002.8838	672.8202	452.6637
2.7500	3710.5836	2353.8549	1542.7631	1027.1420	688.8890	463.4136
2.8000	3816.5297	2413.7376	1579.8262	1051.1273	704.7418	474.0279
2.8500	3922.4758	2473.2167	1616.3597	1074.8346	720.4341	484.4989
2.9000	4028.4219	2532.2792	1652.8381	1098.2630	735.9059	494.8298
2.9500	4134.3679	2590.9473	1688.6694	1121.4115	751.1606	505.0109

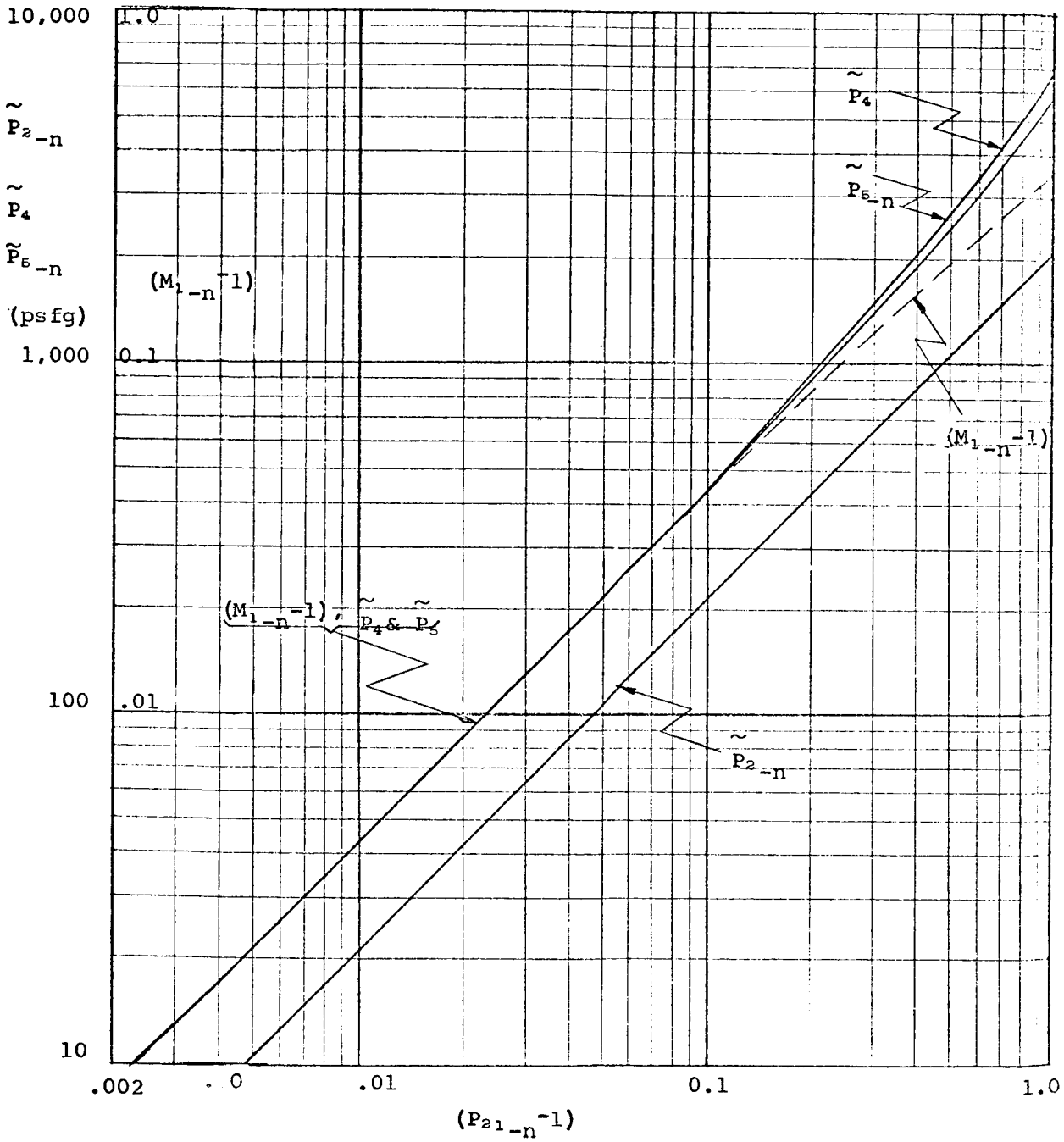

FIGURE 1 - PRESSURES IN WEAK (QUASI-LINEAR) NORMAL SHOCK FLOW

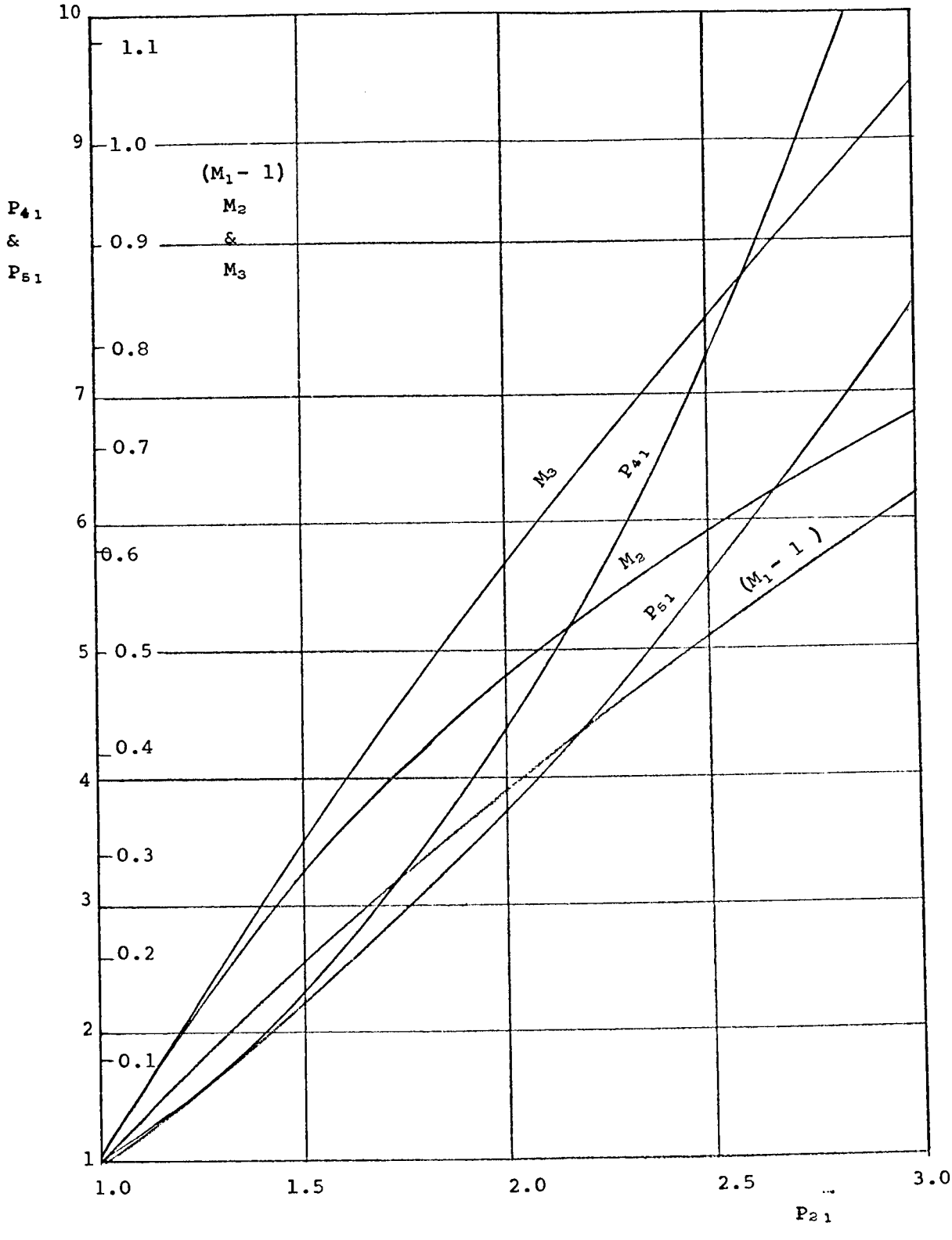

FIGURE 2 - SHOCK TUBE FLOW CHARACTERISTICS

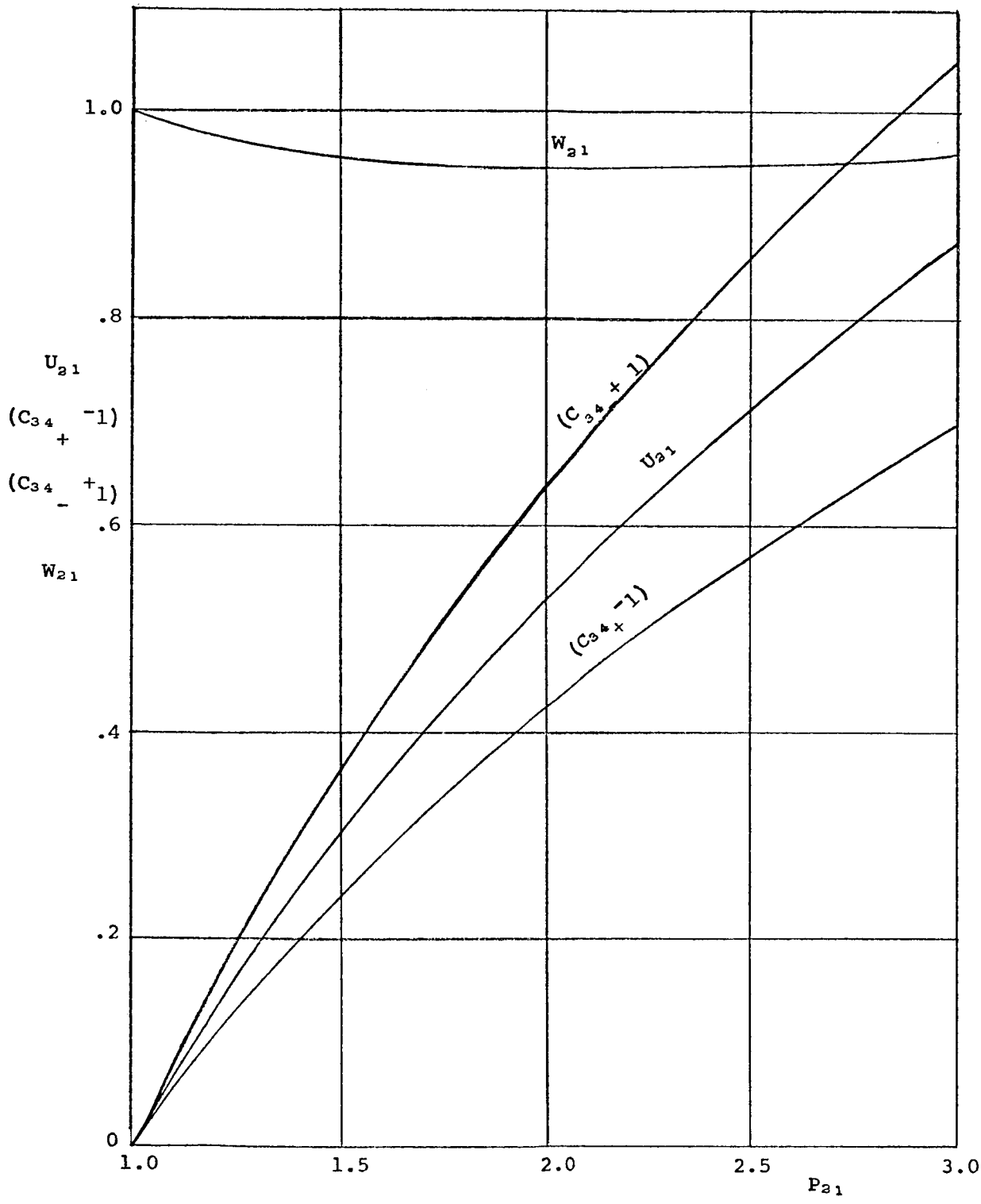

FIGURE 3 - SHOCK TUBE FLOW CHARACTERISTICS

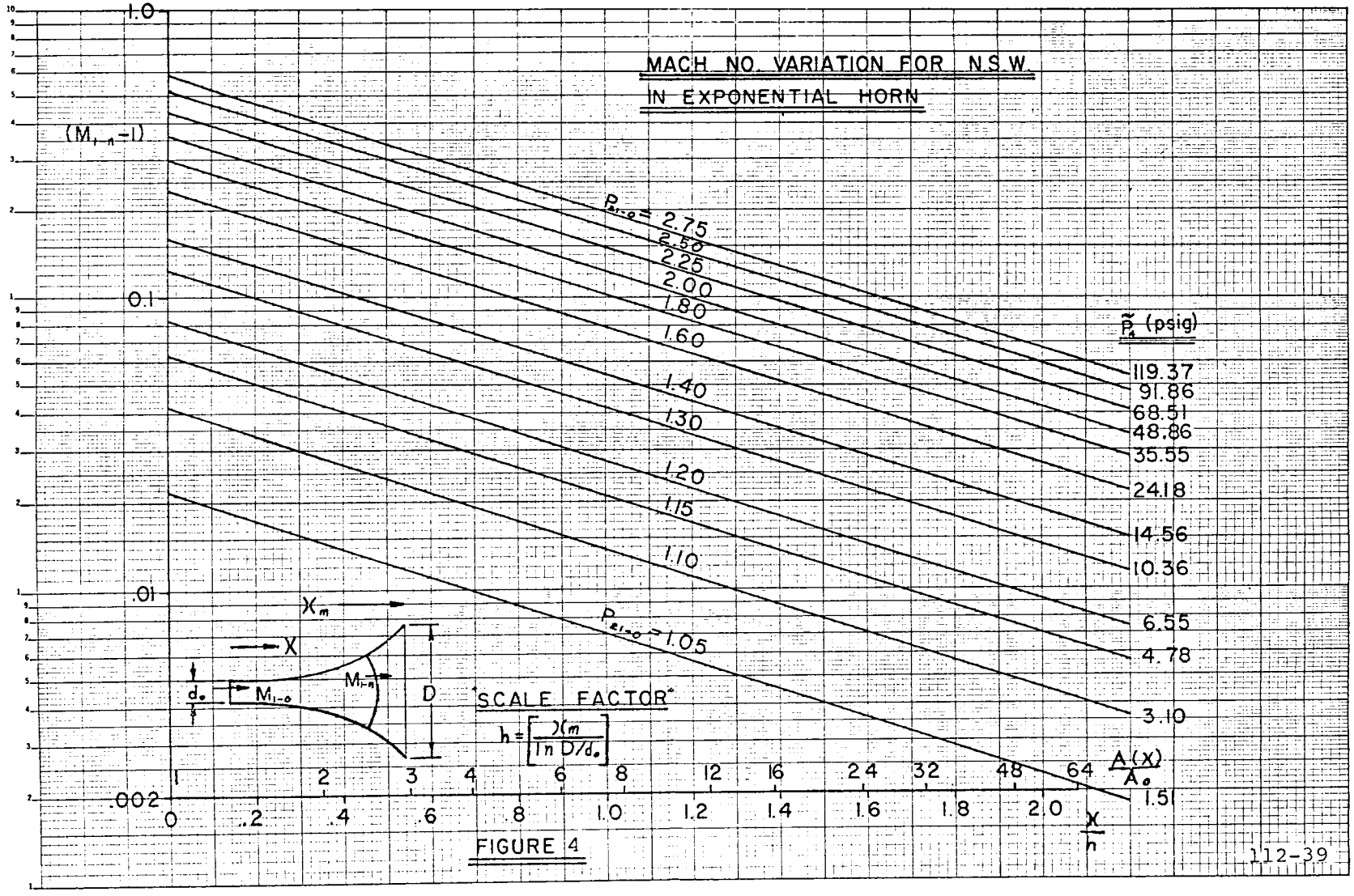

FIGURE 4

112-39

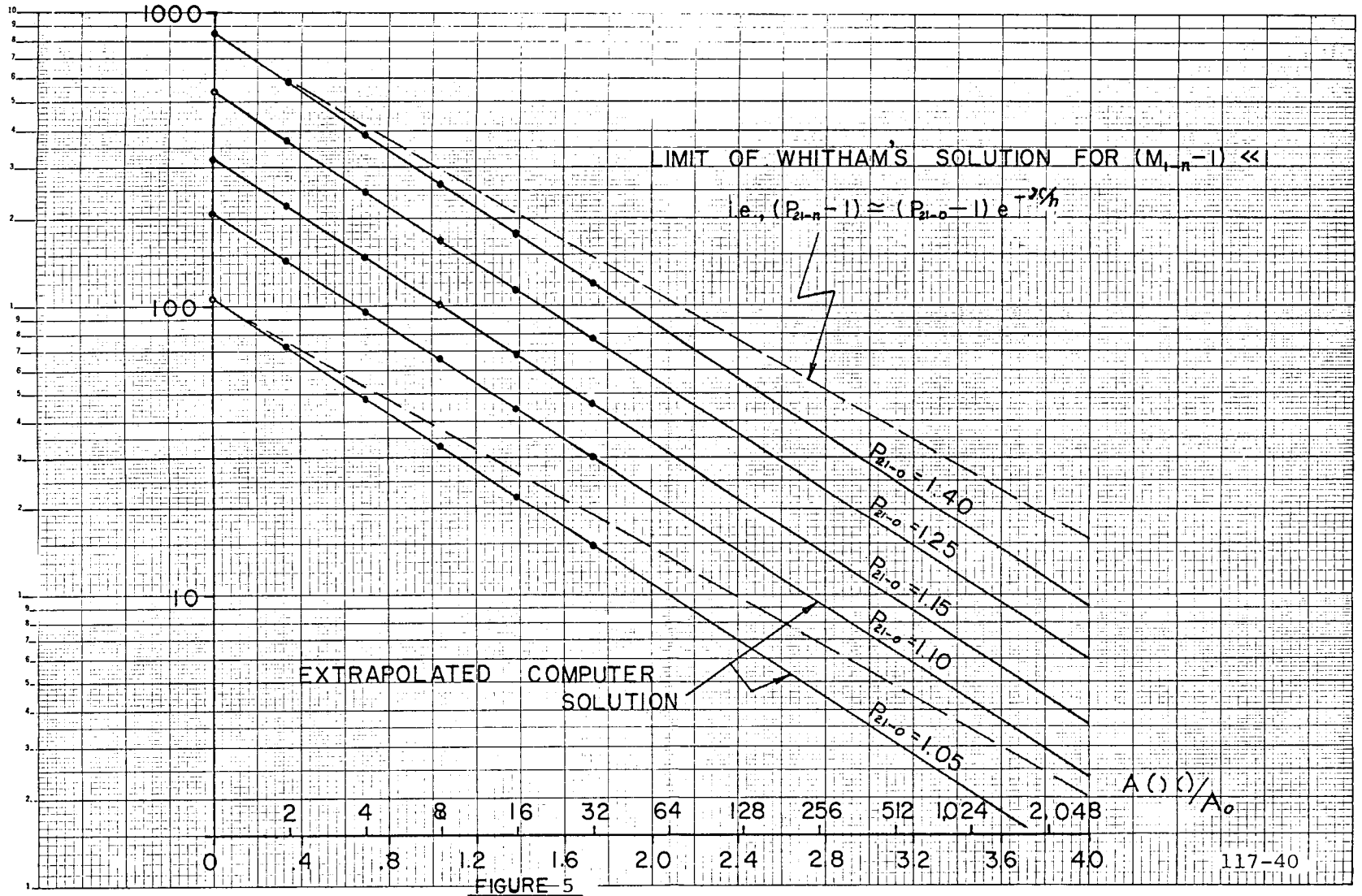
1000
100
10
LIMIT OF WHITHAM'S SOLUTION FOR $(M_{1-n}-1) \ll$
i.e., $(P_{21-n}-1) \simeq (P_{21-o}-1)\, e^{-2C/h}$
$P_{21-o}=1.40$
$P_{21-o}=1.25$
$P_{21-o}=1.15$
$P_{21-o}=1.10$
$P_{21-o}=1.05$
EXTRAPOLATED COMPUTER SOLUTION
$A_{(\ )(\ )}/A_o$
2
4
8
16
32
64
128
256
512
1,024
2,048
0
.4
.8
1.2
1.6
2.0
2.4
2.8
3.2
3.6
4.0
117-40

FIGURE-5

APPENDIX II

LIST OF SYMBOLS

A_n = Area in the expansion region at station n

A_0 = Cross-sectional area of the shock tube and acoustic horn throat

a_i = Speed of sound in flow region i

C_{34+} = Reflected rarefaction wave leading edge velocity

C_{34-} = Rarefaction wave trailing edge velocity

C_{44} = Rarefaction wave leading edge velocity

h = Incremental change in expansion ratio selected for numerical integration

$K_{n-1} = 2\left[\left(1 + \frac{2}{\gamma+1}\right)\left(\frac{1-\mu^2}{\mu}\right)\left(2\mu + 1 + M^{-2}\right)\right]$

where $\mu^2 = \frac{(\gamma-1)\,M^2 + 2}{2\gamma M^2 - (\gamma-1)}$

L = Driver section length

M_{1-0} = Driven section Mach number of primary shock wave

$(M)_n, M_{1-n}$ = Shock wave Mach number in the expansion region at station n

$\tilde{P}_4$ = Gauge pressure, lb/ft^2 or lb/in^2

P_{14} = Ratio of driven section pressure to driver section pressure prior to diaphragm burst

P_{21} = Ratio of upstream to downstream pressure across the primary shock wave

P_{21-n} = Ratio of upstream to downstream pressure across the primary shock in the expansion region at station n

T = Nondimensionalized time

t = Time

u_i = Particle velocity in region i

U_{21} = Ratio of driver gas velocity to ambient sound speed in region 1

w_2 = Local wave speed (relative to the medium) in region 2

W_{21} = Mach number of normally reflected shock wave

X = Nondimensionalized position

x = Axial position in the shock tube/horn combination as measured from the diaphragm location

γ = Ratio of specific heat

"The aeronautical and space activities of the United States shall be conducted so as to contribute . . . to the expansion of human knowledge of phenomena in the atmosphere and space. The Administration shall provide for the widest practicable and appropriate dissemination of information concerning its activities and the results thereof."

—NATIONAL AERONAUTICS AND SPACE ACT OF 1958

NASA SCIENTIFIC AND TECHNICAL PUBLICATIONS

TECHNICAL REPORTS: Scientific and technical information considered important, complete, and a lasting contribution to existing knowledge.

TECHNICAL NOTES: Information less broad in scope but nevertheless of importance as a contribution to existing knowledge.

TECHNICAL MEMORANDUMS: Information receiving limited distribution because of preliminary data, security classification, or other reasons.

CONTRACTOR REPORTS: Scientific and technical information generated under a NASA contract or grant and considered an important contribution to existing knowledge.

TECHNICAL TRANSLATIONS: Information published in a foreign language considered to merit NASA distribution in English.

SPECIAL PUBLICATIONS: Information derived from or of value to NASA activities. Publications include conference proceedings, monographs, data compilations, handbooks, sourcebooks, and special bibliographies.

TECHNOLOGY UTILIZATION PUBLICATIONS: Information on technology used by NASA that may be of particular interest in commercial and other non-aerospace applications. Publications include Tech Briefs, Technology Utilization Reports and Notes, and Technology Surveys.

Details on the availability of these publications may be obtained from:

SCIENTIFIC AND TECHNICAL INFORMATION DIVISION

NATIONAL AERONAUTICS AND SPACE ADMINISTRATION

Washington, D.C. 20546